

State-Selective Signatures of Quantum and Classical Gravitational Environments

Partha Nandi,^{1,2,*} Sankarshan Sahu,^{3,†} Bibhas Ranjan Majhi,^{4,‡} and Francesco Petruccione^{2,5,§}

¹*Department of Physics, University of Stellenbosch, Stellenbosch, 7600, South Africa*

²*National Institute of Theoretical and Computational Sciences (NITheCS), Stellenbosch, 7604, South Africa*

³*Sorbonne Université, CNRS, Laboratoire de Physique Théorique de la Matière Condensée, LPTMC, 75005 Paris, France*

⁴*Department of Physics, Indian Institute of Technology Guwahati, Guwahati 781039, Assam, India*

⁵*School of Data Science and Computational Thinking,
University of Stellenbosch, Stellenbosch 7600, South Africa*

(Dated: March 9, 2026)

A unified framework is developed for determining whether a gravitational-wave (GW) background behaves as a classical field or as a genuinely quantum environment. *Unified* here means that both descriptions originate from the same tidal coupling derived from geodesic deviation, which yields an identical quadratic interaction Hamiltonian for the detector; the only distinction lies in whether the GW degrees of freedom are modeled as classical phase-randomized coherent states or as quantized graviton modes. Within this common framework, the reduced dynamics of a quantum harmonic oscillator exhibit a sharp structural contrast: a quantized graviton bath preserves coherence within the lowest phonon-number manifold, forming a protected sector at leading order, whereas a classical stochastic GW field inevitably induces decoherence even inside this subspace. This difference provides an operational criterion for diagnosing the classical or quantum nature of gravitational waves using mesoscopic optomechanical systems. Our results establish decoherence structure—not merely its magnitude—as a sensitive probe of gravitational quantumness and delineate the experimental regimes under which such tests may become feasible.

I. INTRODUCTION

The first direct detection of gravitational waves by LIGO in 2015 [1, 2] confirmed the predictions of Einstein’s general relativity with remarkable precision and established gravitational radiation as a tangible physical reality. Yet a deeper question persists: do gravitational waves themselves admit a fundamentally quantum description, and if so, can this be established operationally? More generally, the interpretation of quantum states of the gravitational field can be subtle: configurations that appear as superpositions of spacetime geometries may in some cases admit equivalent descriptions on a single classical background with appropriately transformed quantum degrees of freedom [3]. This issue lies at the heart of the interface between quantum mechanics and gravitation.

In practice, the statement that “gravitational waves are classical” is typically understood to mean that the radiation field can be described by coherent states with large occupation numbers, which represent the quantum states that most closely resemble classical wave configurations [4]. In quantum optics, coherent states exhibit minimal quantum fluctuations and the field operators act effectively as c -numbers in expectation values, reproducing the behavior of classical radiation fields. From this perspective, deviations from coherent-state statistics—such as thermal, squeezed, or other nonclassical states—would

signal intrinsically quantum features of gravitational radiation.

This viewpoint has recently been sharpened by Manikandan and Wilczek, who proposed operational tests of the coherent-state hypothesis using resonant bar detectors and counting statistics [5, 6]. Their analysis highlights that departures from coherent-state behavior could provide direct evidence for a quantum structure underlying gravitational waves.

In the present work, we adopt a complementary dynamical perspective. Rather than analyzing the counting statistics of the gravitational field itself, we investigate how a mesoscopic quantum system [7] evolves when coupled to a gravitational-wave background. Within the framework of open quantum systems [8], the gravitational field plays the role of an environment whose microscopic nature—whether a classical stochastic field or a quantized graviton bath—can imprint distinct structural signatures on the reduced dynamics of a quantum probe.

More generally, connections between coherent-state phase-space representations and effective hydrodynamic descriptions of quantum dynamics have long been recognized. As an illustrative example, Ghosh *et al.* showed that the Schrödinger equation can be mapped to Euler and Navier–Stokes–type equations in a coherent-state representation when environmental modes are included [9]. This perspective highlights how coupling to unobserved degrees of freedom can induce effective dissipative dynamics even in fundamentally quantum systems.

Related open-system formulations have been employed to study decoherence induced by stochastic fluctuations of quantum spacetime, where Planck-scale geometric noise acts as an effective environment for quantum systems [10]. Open-system ideas have also been explored

* pnandi@sun.ac.za

† sankarshan.sahu@sorbonne-universite.fr

‡ bibhas.majhi@iitg.ac.in

§ petruccione@sun.ac.za

in cosmological contexts, where tracing over inhomogeneous fluctuations can render the homogeneous sector effectively open and lead to the emergence of dark-sector components from quantum openness [11]. In parallel, stochastic formulations of quantum gravity have been investigated in which geometric degrees of freedom may arise from probabilistic processes on underlying microscopic structures [12]. Gravity-induced decoherence and entanglement redistribution in many-body gravitational systems have likewise been studied in various contexts [13, 14] (see also [15–18]).

These developments are conceptually related to the broader framework of semiclassical gravity, where quantum fields propagate on a classical spacetime and the geometry evolves according to the expectation value of the stress–energy tensor [19]. Within this picture, quantum fluctuations of matter fields can influence the effective spacetime dynamics even when the gravitational sector itself is treated classically.

Our aim is to formulate and analyze this scenario in a minimal yet experimentally relevant setting, focusing on qualitative differences in the structure of decoherence rather than on the absolute magnitude of decoherence rates.

Direct probes of gravitational-wave–induced motion face fundamental limitations. Even in advanced interferometers such as LIGO, a strain $h \sim 10^{-21}$ displaces a 40 kg mirror by only $\sim 10^{-18}$ m, comparable to quantum and technical noise levels [20–23]. For realistic astrophysical backgrounds ($h \sim 10^{-23}$ – 10^{-26}), the induced displacement becomes many orders of magnitude smaller than the mirror’s zero-point fluctuations, making displacement-based access to quantum features of gravity essentially impossible.

Mesoscopic mechanical systems offer a conceptually different opportunity. Levitated or optomechanical resonators can act as high-sensitivity probes of weak forces and have been proposed as detectors of high-frequency gravitational waves [24]. Although the GW-induced displacement of a micron-scale resonator is likewise extremely small—far below its zero-point amplitude—the key advantage of mesoscopic platforms lies in their ability to prepare and measure well-defined quantum states of motion. State-of-the-art optomechanical membranes, phononic-crystal resonators, and circuit-QED hybrids can access the lowest phonon-number manifolds [25–29], enabling coherence-based probes of gravitational physics rather than displacement sensing.

To illustrate the scale, consider a GHz resonator such as a high-overtone bulk acoustic resonator (HBAR) [30] or an optomechanical crystal (OMC) [25–27] with a characteristic mode length $L \lesssim 1 \mu\text{m}$. In a representative HBAR device, the mechanical mode has $\omega/2\pi \simeq 5.96$ GHz and effective mass $m_{\text{eff}} \simeq 16.2 \mu\text{g}$, yielding a zero-point amplitude $x_{\text{zpf}} \simeq 2.9 \times 10^{-19}$ m for this particular GHz-scale device [31]. In other optomechanical platforms with smaller masses and lower frequencies, the zero-point displacement can be significantly

larger (typically $x_{\text{zpf}} \sim 10^{-17}$ m), bringing it closer to gravitational-wave strain scales. For representative gravitational-wave strain amplitudes (e.g. $h \sim 10^{-23}$), the direct GW-induced displacement $\Delta x_{\text{GW}} = hL$ is therefore only $\sim 10^{-29}$ m for micron-scale devices, so that $\Delta x_{\text{GW}}/x_{\text{zpf}} \sim 10^{-11}$. Such signals are far too small to classicalize the oscillator or populate phonons; the device therefore remains fully quantum. In this regime, the relevant signature of the gravitational environment is not the displacement amplitude but its *statistical structure*.

Motivated by these developments, we model the detector as a generic quantum mechanical resonator—formally, a single quantum harmonic oscillator mode coupled to a gravitational-wave background [22, 23, 32–34]. Within a unified open-quantum-system framework, we compare two physically distinct descriptions of the gravitational field:

1. **Quantum gravitational waves:** the gravitational field is treated as a Gaussian quantum environment, taken either in the vacuum state or in an effective thermal (Gibbs) state. Here the term “thermal” refers to the form of the quantum density matrix and does not imply ongoing graviton thermalization through interactions [35]. Such a state may arise, for example, as a relic of early-universe initial conditions (e.g. a radiation-dominated era preceding inflation [36, 37]), or may be employed as a convenient parametrization of Gaussian quantum fluctuations.
2. **Classical gravitational waves:** the gravitational field is modeled as a classical stochastic background, represented by an ensemble of phase-randomized coherent states. This description captures incoherent superpositions of classical gravitational waves emitted by many independent sources and provides a natural classical noise limit of the theory.

The choice of gravitational field states is motivated by the distinct physical regimes they represent. A pure coherent state of the graviton field possesses a nonvanishing expectation value $\langle h_{ij} \rangle$ and thus corresponds to a deterministic classical gravitational wave [4]. Thermal and phase-randomized coherent states, by contrast, have vanishing one-point functions but nonzero two-point correlators, capturing stochastic gravitational-wave backgrounds with either quantum or classical origin. Within the same microscopic detector–gravity coupling, these different field states give rise to qualitatively distinct reduced dynamics for the harmonic oscillator. In particular, the structure of the induced master equation—and the existence or absence of protected subspaces—allows one to distinguish between quantum-vacuum fluctuations and classical stochastic gravitational noise, without relying solely on the magnitude of decoherence rates.

In both cases, the interaction arises from the same geodesic-deviation tidal coupling, leading to an identi-

cal quadratic detector–gravity Hamiltonian; the difference lies solely in the statistical properties of the gravitational sector. Building on this unified starting point, we derive the associated master equations and analyze their dynamics using perturbative and Liouvillian techniques. Our central result is that, for a quantized graviton field in the vacuum state, the reduced dynamics exhibits a Fock-space *protected subspace*, within which coherence in the lowest phonon-number manifold is preserved at leading order. This protection is absent for classical phase-randomized backgrounds and is also lifted in the presence of finite graviton occupation (e.g. thermal states), where decoherence becomes unavoidable. This sharp structural distinction provides a clear operational method for discriminating between classical and genuinely quantum-vacuum gravitational fluctuations using mesoscopic mechanical probes. In addition, by estimating the magnitude of graviton-induced decoherence for realistic GHz mechanical platforms, we derive model-independent bounds on possible non-vacuum graviton occupation numbers at the detector frequency.

Organization of the paper. Section II introduces the oscillator–gravitational-wave interaction and derives the effective Hamiltonian. Section III formulates the open-system dynamics for a quantized graviton bath. Section IV analyzes the decoherence produced by a classical, phase-randomized background and contrasts it with the quantum case. Sections V and VI discuss experimental implications, coherence-time estimates, and prospects for detection. Appendices provide supporting derivations and technical details.

II. QUANTUM MECHANICS ON A GRAVITATIONAL BACKGROUND

We consider weak gravitational waves propagating on a flat Minkowski background. The spacetime metric is written as

$$g_{\mu\nu} = \eta_{\mu\nu} + h_{\mu\nu}, \quad |h_{\mu\nu}| \ll 1, \quad (1)$$

where $h_{\mu\nu}$ is a small perturbation around the flat metric $\eta_{\mu\nu}$. In the *transverse–traceless* (TT) gauge, the physical degrees of freedom are isolated by imposing

$$h_{0\mu} = 0, \quad \partial^i h_{ij} = 0, \quad h^i{}_i = 0. \quad (2)$$

Under these conditions, the quadratic (free) Einstein–Hilbert action becomes

$$S_{\text{grav}} = \frac{1}{64\pi G} \int d^4x (\dot{h}_{ij}\dot{h}^{ij} - \partial_k h_{ij} \partial_k h^{ij}), \quad (3)$$

describing two tensorial modes satisfying the vacuum wave equation

$$\square h_{ij}^{TT}(t, \vec{x}) = 0, \quad i, j = 1, 2, 3, \quad (4)$$

corresponding to freely propagating gravitational waves with “+” and “×” polarizations.

To analyze the interaction of gravitational waves with matter, we consider a congruence of timelike geodesics $x^\mu(\tau)$ centered around a freely falling detector. The analysis is performed in the *proper detector frame*, a locally inertial coordinate system constructed along the detector’s worldline [38]. In this frame, the metric is locally Minkowskian at the origin, while curvature effects manifest as tidal forces proportional to spatial separations. The four-velocity of the detector is $u^\mu = (1, 0, 0, 0)$, and the spatial separation vector ξ^μ , defined by $\xi^\mu u_\mu = 0$, represents the physical displacement between nearby geodesics [39].

The relative acceleration between neighboring geodesics is given by the geodesic deviation equation [40]:

$$\frac{D^2 \xi^\mu}{D\tau^2} = -R^\mu{}_{\nu\rho\sigma} \xi^\rho u^\nu u^\sigma, \quad (5)$$

where $D/D\tau$ denotes the covariant derivative along the trajectory. In the weak-field limit, the Riemann tensor is linear in $h_{\mu\nu}$:

$$R^\mu{}_{\rho\sigma\nu} = \frac{1}{2} \eta^{\mu\lambda} (\partial_\sigma \partial_\rho h_{\nu\lambda} - \partial_\sigma \partial_\lambda h_{\nu\rho} - \partial_\nu \partial_\rho h_{\sigma\lambda} + \partial_\nu \partial_\lambda h_{\sigma\rho}). \quad (6)$$

In the *long-wavelength approximation*, valid when the gravitational wavelength is much larger than the detector size, spatial variations can be neglected:

$$h_{ij}^{TT}(t, \vec{x}) \simeq h_{ij}^{TT}(t). \quad (7)$$

Substituting this into Eq. (5) and working in the detector frame yields

$$\frac{d^2 \xi^i}{dt^2} = \frac{1}{2} \ddot{h}_{ij}^{TT}(t) \xi^j, \quad (8)$$

where we have used

$$R^j{}_{0k0} = -\frac{1}{2} \ddot{h}_{jk}^{TT}(t). \quad (9)$$

For a gravitational wave propagating along the z -axis, the perturbation can be expressed as

$$h_{ij}^{TT}(t) = \chi(t) (\epsilon_\times \sigma_{ij}^1 + \epsilon_+ \sigma_{ij}^3), \quad (10)$$

where $\chi(t)$ represents the time-dependent amplitude and $\epsilon_\times, \epsilon_+$ are the polarization components associated with the standard basis tensors σ_{ij}^1 and σ_{ij}^3 , the components of Pauli matrices.

To describe the response of a realistic detector, we consider a mesoscopic optomechanical mirror [41] whose center-of-mass (COM) displacement $\xi_1(t)$ along the x -axis experiences both optical trapping and gravitationally induced tidal accelerations. We project the dynamics onto the mechanically relevant center-of-mass mode along the $\xi_1(t)$ -axis; for a gravitational wave propagating along z , the \times polarization does not excite this mode at linear order in the absence of transverse displacement,

and quantum fluctuations in orthogonal directions are neglected as they do not couple to the readout channel [42].

In Fermi normal coordinates centered at the optical trap, the mirror obeys

$$m_0 \ddot{\xi}_1(t) + m_0 \omega_c^2 \xi_1(t) = \frac{m_0}{2} \ddot{h}_{11}^{TT}(t) \xi_1(t), \quad (11)$$

where m_0 is the mirror mass and ω_c the trapping frequency. The corresponding effective Hamiltonian is

$$\begin{aligned} H_D &= \frac{1}{2m_0} \left[p_1 + m_0 \dot{h}_{11}^{TT}(t) \xi_1 \right]^2 + \frac{1}{2} m_0 \omega_c^2 \xi_1^2 \\ &\simeq \frac{p_1^2}{2m_0} + \dot{h}_{11}^{TT}(t) \xi_1 p_1 + \frac{1}{2} m_0 \omega_c^2 \xi_1^2, \end{aligned} \quad (12)$$

where p_1 denotes the canonical momentum. This Hamiltonian, first introduced in [43] and later used in quantum-gravity-inspired detector models [44, 45], forms the basis for our subsequent quantum analysis of the mirror's motion in a gravitational-wave background.

In large-scale detectors such as LIGO, the end mirrors are suspended pendulums with masses around $m_0 \sim 40$ kg and fundamental suspension frequencies near $\omega_0 \sim 0.74$ Hz [20]. The gravitational-wave-induced displacements ($\sim 10^{-18}$ m) are about an order of magnitude larger than the quantum zero-point fluctuations, yet the mirror's high thermal occupation suppresses any observable quantum signatures. Consequently, mirror motion in LIGO is accurately modeled classically, and intrinsically quantum effects—such as gravitationally induced Aharonov–Bohm–type phase shifts—remain undetectable. In contrast, mesoscopic optomechanical systems employ oscillators with effective masses $m_0 \sim 10^{-12}$ – 10^{-9} kg and frequencies $\omega_c \sim 10^5$ – 10^6 rad/s [46–48]. Their quantum zero-point displacement,

$$\Delta x_{\text{zpf}} = \sqrt{\frac{\hbar}{2m_0\omega_c}}, \quad (13)$$

typically reaches $\Delta x_{\text{zpf}} \sim 10^{-17}$ m, comparable to expected gravitational-wave strains. State-of-the-art experiments [26, 27, 46, 49] achieve near-ground-state cooling ($\langle n \rangle < 1$), providing an experimentally accessible regime where quantum mechanics and weak spacetime curvature can be jointly explored.

Thus, in the weak-field approximation, the dynamics of a mesoscopic quantum system under a GW traveling along the z -axis is governed by the time-dependent Hamiltonian [22]:

$$\hat{H}(t) = \left(\alpha \hat{p}_1^2 + \beta \hat{\xi}_1^2 \right) + \gamma(t) \left(\hat{\xi}_1 \hat{p}_1 + \hat{p}_1 \hat{\xi}_1 \right), \quad (14)$$

where $\alpha = 1/(2m_0)$, $\beta = (1/2)m_0\omega_c^2$, $\gamma(t) = \frac{\dot{h}_{11}^{TT}(t)}{2} \epsilon_+$.

III. OPEN QUANTUM GRAVITON ENVIRONMENT: MASTER EQUATION

The interaction between a mesoscopic quantum system—modeled here as a single mechanical mode described by a quantum harmonic oscillator—and a quantized gravitational environment induces effective open-system dynamics. In this section, we derive the corresponding master equation governing the decoherence of the detector due to its coupling with an environment of quantized, plus-polarized gravitational wave modes (gravitons).

We begin with the total Hamiltonian,

$$\begin{aligned} \hat{H} &= \underbrace{\sum_k \hbar \omega_k^g : \hat{b}_k^\dagger \hat{b}_k :}_{\hat{H}_g} \otimes \mathbf{I}_d + \mathbf{I}_g \otimes \underbrace{\hbar \omega_c \left(\hat{a}_1^\dagger \hat{a}_1 + \frac{1}{2} \right)}_{\hat{H}_d} \\ &\quad + i \hbar \underbrace{\sum_k \gamma^k(t) \otimes (\hat{a}_1^{\dagger 2} - \hat{a}_1^2)}_{\hat{H}_{\text{int}}(t)}. \end{aligned} \quad (15)$$

Here, \hat{H}_g and \hat{H}_d denote the free Hamiltonians of the gravitational field and the detector, respectively, while $\hat{H}_{\text{int}}(t)$ describes their interaction. The quantity ω_k^g is the angular frequency of the k^{th} mode of the linearized gravitational field (graviton), and ω_c is the natural frequency of the detector, modeled as a single quantum harmonic oscillator mode. The operators \hat{b}_k and \hat{b}_k^\dagger are the annihilation and creation operators of the graviton modes, satisfying bosonic commutation relations, while \hat{a}_1 and \hat{a}_1^\dagger are the corresponding annihilation and creation operators for the detector mode, obeying the standard bosonic Fock algebra. Normal ordering is employed in \hat{H}_g to remove the irrelevant vacuum energy contribution of the graviton field, thereby avoiding unphysical divergences (see Appendix A for details). The interaction coefficient $\gamma^k(t)$ is defined as

$$\gamma^k(t) = i C_{\omega_k^g} \left(\hat{b}_k^\dagger e^{i\omega_k^g t} - \hat{b}_k e^{-i\omega_k^g t} \right), \quad C_{\omega_k^g} = \frac{C_{\omega_k^g}}{\sqrt{L^3}}, \quad (16)$$

where $C_{\omega_k^g} = \sqrt{\frac{\omega_k^g c l_p^2}{2}}$.

Passing to the interaction picture with respect to the free Hamiltonian $\hat{H}_0 = \hat{H}_g + \hat{H}_d$, the interaction Hamiltonian becomes

$$\begin{aligned} \hat{H}_{\text{int}}^I(t) &= \hbar \sum_k C_{\omega_k^g} \left[\hat{b}_k \hat{a}_1^{\dagger 2} e^{i(2\omega_c - 2\omega_k^g)t} - \hat{b}_k \hat{a}_1^2 e^{-i(2\omega_c + 2\omega_k^g)t} \right. \\ &\quad \left. + \hat{b}_k^\dagger \hat{a}_1^2 e^{i(2\omega_k^g - 2\omega_c)t} - \hat{b}_k^\dagger \hat{a}_1^{\dagger 2} e^{i(2\omega_c + 2\omega_k^g)t} \right]. \end{aligned} \quad (17)$$

This expression follows from the standard interaction-picture transformation

$$\hat{H}_{\text{int}}^I(t) = e^{\frac{i}{\hbar}(\hat{H}_g + \hat{H}_d)t} \hat{H}_{\text{int}}(t) e^{-\frac{i}{\hbar}(\hat{H}_g + \hat{H}_d)t}. \quad (18)$$

The time evolution of the total density matrix is governed by the von-Neumann equation,

$$\frac{d}{dt}\hat{\rho}^{\text{tot}}(t) = -\frac{i}{\hbar}[\hat{H}_{\text{int}}^I(t), \hat{\rho}^{\text{tot}}(t)]. \quad (19)$$

Formally integrating Eq. (19) gives

$$\hat{\rho}^{\text{tot}}(t) = \hat{\rho}_0^{\text{tot}} - \frac{i}{\hbar} \int_0^t ds [\hat{H}_{\text{int}}^I(s), \hat{\rho}^{\text{tot}}(s)], \quad (20)$$

which, upon substitution, yields

$$\begin{aligned} \frac{d}{dt}\hat{\rho}^{\text{tot}}(t) &= -\frac{i}{\hbar}[\hat{H}_{\text{int}}^I(t), \hat{\rho}_0^{\text{tot}}] \\ &\quad - \frac{1}{\hbar^2} \int_0^t ds [\hat{H}_{\text{int}}^I(t), [\hat{H}_{\text{int}}^I(s), \hat{\rho}^{\text{tot}}(s)]]. \end{aligned} \quad (21)$$

In the above $\hat{\rho}_0^{\text{tot}}$ is the initial composite density matrix.

Applying the Born approximation (i.e. the interaction between the graviton modes and the detector is very weak, so that $\hat{\rho}^{\text{tot}}(s) \approx \hat{\rho}_d(s) \otimes \rho_g$), and then tracing over the gravitational field degrees of freedom, we obtain

$$\frac{d}{dt}\hat{\rho}_d(t) = -\frac{1}{\hbar^2} \int_0^t ds \text{Tr}_g \left[\hat{H}_{\text{int}}^I(t), [\hat{H}_{\text{int}}^I(s), \hat{\rho}_d(s) \otimes \rho_g] \right]. \quad (22)$$

The first-order contribution $\text{Tr}_g [\hat{H}_{\text{int}}^I(t), \hat{\rho}_0^{\text{tot}}]$ vanishes under the standard assumption that the initial total state is factorized, $\hat{\rho}_0^{\text{tot}} = \hat{\rho}_d(0) \otimes \rho_g$, and that the gravitational environment has vanishing first moments, $\text{Tr}_g(\hat{b}_k \rho_g) = \text{Tr}_g(\hat{b}_k^\dagger \rho_g) = 0$. Since the interaction Hamiltonian (17) is linear in the graviton operators \hat{b}_k and \hat{b}_k^\dagger , the trace over the gravitational sector produces expectation values of these operators, all of which vanish for vacuum and thermal states. Consequently,

$$\text{Tr}_g [\hat{H}_{\text{int}}^I(t), \hat{\rho}_0^{\text{tot}}] = 0, \quad (23)$$

and the leading contribution to the reduced dynamics arises at second order in the interaction.

Extending the upper integration limit to $t \rightarrow \infty$, the master equation in the Born–Markov approximation becomes

$$\frac{d}{dt}\hat{\rho}_d(t) = -\frac{1}{\hbar^2} \int_0^\infty ds \text{Tr}_g \left[\hat{H}_{\text{int}}^I(t), [\hat{H}_{\text{int}}^I(t-s), \hat{\rho}_d(t) \otimes \rho_g] \right], \quad (24)$$

where the graviton thermal state is

$$\rho_g \rightarrow \rho_g^{\text{th}} = \frac{e^{-\beta_g \hat{H}_G}}{\text{tr}(e^{-\beta_g \hat{H}_G})}. \quad (25)$$

Furthermore, this allows us to compute the explicit form of the thermal correlation functions for the following bilinears:

$$\begin{aligned} \langle \hat{b}_l^\dagger \hat{b}_m^\dagger \rangle_g &= 0, & \langle \hat{b}_l \hat{b}_m \rangle_g &= 0, \\ \langle \hat{b}_l^\dagger \hat{b}_m \rangle_g &= \delta_{lm} \bar{n}_l, & \langle \hat{b}_l \hat{b}_m^\dagger \rangle_g &= \delta_{lm} (1 + \bar{n}_l), \\ \langle \hat{b}_l^\dagger \hat{b}_m^\dagger \rangle_g^* &= 0, & \langle \hat{b}_l \hat{b}_m \rangle_g^* &= 0, \\ \langle \hat{b}_l^\dagger \hat{b}_m \rangle_g^* &= \delta_{lm} (1 + \bar{n}_l), & \langle \hat{b}_l \hat{b}_m^\dagger \rangle_g &= \delta_{lm} \bar{n}_l. \end{aligned} \quad (26)$$

where the expectation value is taken over the graviton thermal state, where $\langle \hat{A} \hat{B} \rangle_g \equiv \text{Tr}_g(\hat{A} \hat{B} \hat{\rho}_g)$, $\langle \hat{A} \hat{B} \rangle_g^* \equiv \text{Tr}_g(\hat{A} \hat{\rho}_g \hat{B})$, and $\bar{n}_l = \frac{1}{e^{\hbar \omega_l^g / k_B T_g} - 1}$ is the thermal occupation number of mode l with $\beta_g = 1/(k_B T_g)$.

Following a standard coarse-graining procedure, we assume that the graviton reservoir modes are closely spaced in frequency and pass to the continuum limit. In a cubic quantization volume $V = L^3$, the discrete momentum sum is replaced by

$$\sum_{\vec{k}} \rightarrow \frac{V}{(2\pi)^3} \int d^3k = \frac{V}{2\pi^2} \int_0^\infty d\omega_g f(\omega_g). \quad (27)$$

where $f(\omega_g)$ denotes the spectral profile of the gravitational reservoir, reducing to $f(\omega_g) = \omega_g^2$ for free gravitons in 3 + 1 dimensions.

Also we use Sokhotski–Plemelj theorem (see Eq. (4.15) of [50])

$$\begin{aligned} \int_0^\infty ds e^{\pm i(2\omega_l^g - 2\omega_c)s} &= \pi \delta(\omega_l^g - \omega_c) \\ &\quad - i\mathcal{P}\left(\frac{1}{2(\omega_l^g - \omega_c)}\right), \end{aligned} \quad (28)$$

where \mathcal{P} represents the principal value. Now in the Markovian regime, the Dirac-delta contribution dominates because it corresponds to real, energy-conserving transitions, while the principal-value term represents virtual off-resonant processes whose net effect is only a small frequency shift. This yields, for the term containing the nested commutator in Eq. (24),

$$\begin{aligned} \int_0^\infty ds \langle \hat{H}_{\text{int}}(t) \hat{H}_{\text{int}}(t-s) \hat{\rho}_d(t) \rangle_g &= \frac{\pi}{2} \hbar^2 f(\omega_c) C_{\omega_c}^2 \\ &\times \left[(1 + \bar{n}_c) (\hat{a}_1^{\dagger 2} \hat{a}_1^2 \hat{\rho}_d(t) - \hat{a}_1^2 \hat{a}_1^{\dagger 2} \hat{\rho}_d(t) e^{-i4\omega_c t}) + \right. \\ &\quad \left. \bar{n}_c (\hat{a}_1^2 \hat{a}_1^{\dagger 2} \hat{\rho}_d(t) - \hat{a}_1^{\dagger 2} \hat{a}_1^2 \hat{\rho}_d(t) e^{i4\omega_c t}) \right], \end{aligned} \quad (29)$$

where $f(\omega_c)$ denotes the spectral weight of the graviton bath evaluated at the detector frequency ω_c (see Appendix B for details).

Carrying out the analogous steps for the remaining contributions in Eq. (24) and collecting all terms, the reduced density matrix in the Schrödinger picture satisfies

$$\frac{d}{dt}\hat{\rho}_d(t) = \mathcal{L}_u \hat{\rho}_d(t) + \mathcal{L}_g \hat{\rho}_d(t), \quad (30)$$

which is equivalent to a Lindblad-type master equation, with \mathcal{L}_u and \mathcal{L}_g denoting the unitary and graviton-induced dissipative contributions, respectively. The unitary part is given by

$$\mathcal{L}_u \hat{\rho}_d(t) = -\frac{i}{\hbar} [\hat{H}_0, \hat{\rho}_d(t)], \quad (31)$$

while the graviton-induced dissipative contribution reads

$$\begin{aligned} \mathcal{L}_g \hat{\rho}_d(t) = & -\frac{\pi}{2} f(\omega_c) C_{\omega_c}^2 \left\{ (1 + \bar{n}_c) \left[\left\{ \hat{a}_1^{\dagger 2} \hat{a}_1^2, \hat{\rho}_d \right\} - 2 \hat{a}_1^2 \hat{\rho}_d(t) \hat{a}_1^{\dagger 2} \right. \right. \\ & \left. \left. + \hat{a}_1^2 \hat{\rho}_d \hat{a}_1^2 e^{-i4\omega_c t} + \hat{a}_1^{\dagger 2} \hat{\rho}_d \hat{a}_1^{\dagger 2} e^{i4\omega_c t} - \hat{a}_1^2 \hat{a}_1^2 \hat{\rho}_d e^{-i4\omega_c t} - \hat{\rho}_d \hat{a}_1^{\dagger 2} \hat{a}_1^{\dagger 2} e^{i4\omega_c t} \right] \right. \\ & \left. + \bar{n}_c \left[\left\{ \hat{a}_1^2 \hat{a}_1^{\dagger 2}, \hat{\rho}_d \right\} - 2 \hat{a}_1^{\dagger 2} \hat{\rho}_d \hat{a}_1^2 + \hat{a}_1^2 \hat{\rho}_d \hat{a}_1^2 e^{-i4\omega_c t} + \hat{a}_1^{\dagger 2} \hat{\rho}_d \hat{a}_1^{\dagger 2} e^{i4\omega_c t} \right. \right. \\ & \left. \left. - \hat{\rho}_d \hat{a}_1^2 \hat{a}_1^2 e^{-i4\omega_c t} - \hat{a}_1^{\dagger 2} \hat{a}_1^{\dagger 2} \hat{\rho}_d e^{i4\omega_c t} \right] \right\}. \quad (32) \end{aligned}$$

To study the decoherence induced by the graviton environment, we now solve the master equation (30) perturbatively to leading order in the gravitational interaction. Formally, the solution of Eq. (30) can be written as

$$\hat{\rho}_d(t) = \hat{\Phi}(t) \hat{\rho}_d(0), \quad (33)$$

where the dynamical map $\hat{\Phi}(t)$ satisfies

$$\hat{\Phi}(t) = e^{\mathcal{L}_u t} \left[1 + \int_0^t d\tau e^{-\mathcal{L}_u \tau} \mathcal{L}_g \hat{\Phi}(\tau) \right]. \quad (34)$$

To first order in \mathcal{L}_g , this expression reduces to

$$\hat{\Phi}(t) \simeq e^{\mathcal{L}_u t} \left[1 + \int_0^t d\tau e^{-\mathcal{L}_u \tau} \mathcal{L}_g e^{\mathcal{L}_u \tau} \right]. \quad (35)$$

This approximation corresponds to treating the graviton-induced dissipative contribution perturbatively, while the unitary evolution generated by \mathcal{L}_u is taken into account exactly. In other words, we work in the interaction picture with respect to \mathcal{L}_u .

Using the explicit form $\mathcal{L}_u \hat{\rho} = -\frac{i}{\hbar} [\hat{H}_0, \hat{\rho}]$, the action of the unitary propagator on an arbitrary operator A is given by

$$e^{\mathcal{L}_u t} A = e^{-\frac{i}{\hbar} \hat{H}_0 t} A e^{\frac{i}{\hbar} \hat{H}_0 t}, \quad (36)$$

which follows directly from the Baker–Campbell–Hausdorff lemma. Consequently, the first-order perturbative solution for the reduced density matrix takes the form

$$\begin{aligned} \hat{\rho}_d(t) = & e^{\mathcal{L}_u t} \hat{\rho}_d(0) \\ & + e^{\mathcal{L}_u t} \int_0^t d\tau e^{\frac{i}{\hbar} \hat{H}_0 \tau} \mathcal{L}_g \left[e^{-\frac{i}{\hbar} \hat{H}_0 \tau} \hat{\rho}_d(0) e^{\frac{i}{\hbar} \hat{H}_0 \tau} \right] e^{-\frac{i}{\hbar} \hat{H}_0 \tau}. \end{aligned} \quad (37)$$

Substituting the explicit form of \mathcal{L}_g , we obtain

$$\begin{aligned} \hat{\rho}_d(t) = & e^{\mathcal{L}_u t} \hat{\rho}_d(0) \\ & - \frac{\pi}{2} f(\omega_c) C_{\omega_c}^2 e^{\mathcal{L}_u t} \int_0^t d\tau \left[(1 + \bar{n}_c) \left\{ \right. \right. \\ & \left. \left. \left\{ \hat{a}_1^{\dagger 2} \hat{a}_1^2, \hat{\rho}_d(0) \right\} - 2 \hat{a}_1^2 \hat{\rho}_d(0) \hat{a}_1^{\dagger 2} - e^{-i4\omega_c \tau} \hat{a}_1^2 \hat{a}_1^2 \hat{\rho}_d(0) \right. \right. \\ & \left. \left. - e^{i4\omega_c \tau} \hat{\rho}_d(0) \hat{a}_1^{\dagger 2} \hat{a}_1^{\dagger 2} + e^{-i4\omega_c \tau} \hat{a}_1^2 \hat{\rho}_d(0) \hat{a}_1^2 \right. \right. \\ & \left. \left. + e^{i4\omega_c \tau} \hat{a}_1^{\dagger 2} \hat{\rho}_d(0) \hat{a}_1^{\dagger 2} \right\} + \bar{n}_c \left\{ \left\{ \hat{a}_1^2 \hat{a}_1^{\dagger 2}, \hat{\rho}_d(0) \right\} \right. \right. \\ & \left. \left. - 2 \hat{a}_1^{\dagger 2} \hat{\rho}_d(0) \hat{a}_1^2 - e^{i4\omega_c \tau} \hat{a}_1^{\dagger 2} \hat{a}_1^{\dagger 2} \hat{\rho}_d(0) \right. \right. \\ & \left. \left. - e^{-i4\omega_c \tau} \hat{\rho}_d(0) \hat{a}_1^2 \hat{a}_1^2 + e^{-i4\omega_c \tau} \hat{a}_1^2 \hat{\rho}_d(0) \hat{a}_1^2 + \right. \right. \\ & \left. \left. \left. e^{i4\omega_c \tau} \hat{a}_1^{\dagger 2} \hat{\rho}_d(0) \hat{a}_1^{\dagger 2} \right\} \right]. \quad (38) \end{aligned}$$

It is worth emphasizing that, throughout this analysis, we deliberately neglect all conventional environmental dissipation channels—such as thermal relaxation, cavity losses, and mechanical damping [51]—in order to isolate decoherence arising solely from the interaction with the gravitational field.

As a first example, consider the initial state $\hat{\rho}_d(0) = |0\rangle\langle 0|$. Using Eq. (38), the corresponding diagonal matrix element evolves, to leading order in the perturbative expansion, as

$$\langle 0 | \hat{\rho}_d(t) | 0 \rangle = 1 - \frac{t}{\tau_G}, \quad \frac{t}{\tau_G} \ll 1, \quad (39)$$

where the characteristic graviton-induced transition time is defined by

$$\tau_G^{-1} = 2\pi \bar{n}_c f(\omega_c) C_{\omega_c}^2. \quad (40)$$

This expression describes graviton-induced excitation out of the ground state and is valid in the short-time regime where the Born–Markov expansion applies.

For comparison, starting from the first excited state $\hat{\rho}_d(0) = |1\rangle\langle 1|$, Eq. (38) yields

$$\langle 1 | \hat{\rho}_d(t) | 1 \rangle = 1 - 3 \frac{t}{\tau_G}, \quad \frac{t}{\tau_G} \ll 1, \quad (41)$$

reflecting the quadratic structure of the detector–gravity coupling. For a quantum-vacuum gravitational environment ($\bar{n}_c = 0$), the rate vanishes identically.

We next consider a coherent superposition of the ground and first excited states,

$$\hat{\rho}_d(0) = \frac{1}{2} (|0\rangle\langle 0| + |0\rangle\langle 1| + |1\rangle\langle 0| + |1\rangle\langle 1|), \quad (42)$$

in order to examine how graviton-induced decoherence affects coherence between energy eigenstates. Applying

Eq. (38), the relevant matrix elements evolve as

$$\langle 0 | \hat{\rho}_d(t) | 0 \rangle = \frac{1}{2} \left(1 - \frac{t}{\tau_G} \right), \quad (43)$$

$$\langle 1 | \hat{\rho}_d(t) | 1 \rangle = \frac{1}{2} \left(1 - 3 \frac{t}{\tau_G} \right), \quad (44)$$

$$\langle 0 | \hat{\rho}_d(t) | 1 \rangle = \frac{1}{2} \left(1 - 2 \frac{t}{\tau_G} \right) e^{i\omega_c t} = \left(\langle 1 | \hat{\rho}_d(t) | 0 \rangle \right)^*. \quad (45)$$

Remarkably, for any initial density matrix supported entirely within the subspace spanned by $\{|0\rangle, |1\rangle\}$ —that is, for any pure state of the form $|\psi(0)\rangle = \alpha_1 |0\rangle + \beta_1 |1\rangle$ with $\alpha_1, \beta_1 \in \mathbb{R}$ —we find that graviton-induced decoherence vanishes in the zero-temperature limit. In this sense, vacuum fluctuations of the linearized gravitational field are effectively *blind* to coherent superpositions within the $\{|0\rangle, |1\rangle\}$ sector: such states remain fully coherent at $T = 0K$, provided all other environmental couplings are suppressed. This behavior changes qualitatively once higher excited states are involved. For example, taking the initial state $\hat{\rho}_d(0) = |2\rangle\langle 2|$ and applying Eq. (38), we obtain

$$\langle 2 | \hat{\rho}_d(t) | 2 \rangle = 1 - 2\pi f(\omega_c) C_{\omega_c}^2 t (1 + 7\bar{n}_c). \quad (46)$$

Equation (46) demonstrates that, unlike the protected $\{|0\rangle, |1\rangle\}$ sector, decoherence persists even in the zero-temperature limit ($\bar{n}_c = 0$).

The introduction of a thermal state for the gravitational field at this stage serves a dual purpose. First, it provides a physically well-defined mixed quantum state that interpolates smoothly between vacuum fluctuations and classical stochastic gravitational-wave noise. In particular, in the high-occupation limit, the thermal graviton state reproduces the field correlators of a classical Gaussian stochastic background, while at low temperatures it retains intrinsically quantum features. Second, unlike the vacuum state, a thermal environment can induce decoherence even when spontaneous emission channels are kinematically suppressed, thereby lifting the protection observed in the $\{|0\rangle, |1\rangle\}$ subspace. In this sense, the thermal graviton bath furnishes a controlled and physically motivated framework for comparing genuinely quantum gravitational fluctuations with their classical stochastic counterpart within a unified open-system description [52]. Such thermal or mixed graviton states may arise, for instance, if inflation is preceded by a radiation-dominated phase, or through stimulated emission during inflation [36, 53], and may also be understood more generally as effective descriptions of stochastic gravitational-wave backgrounds with finite occupation numbers [8, 54].

One can even compute the time evolution of a coherent superposition of the second-excited state with the ground state, i.e. we consider the initial state:

$$\hat{\rho}_d(0) = \frac{1}{2} (|0\rangle\langle 0| + |0\rangle\langle 2| + |2\rangle\langle 0| + |2\rangle\langle 2|), \quad (47)$$

the short-time evolution of the density-matrix elements obtained from Eq. (38) reads

$$\langle 0 | \hat{\rho}_d(t) | 0 \rangle = \frac{1}{2} (1 + 2\pi f(\omega_c) C_{\omega_c}^2 t), \quad (48)$$

$$\langle 2 | \hat{\rho}_d(t) | 2 \rangle = \frac{1}{2} (1 - 2\pi f(\omega_c) C_{\omega_c}^2 t [1 + 6\bar{n}_c]), \quad (49)$$

$$\begin{aligned} \langle 2 | \hat{\rho}_d(t) | 0 \rangle &= \frac{1}{2} (1 - \pi f(\omega_c) C_{\omega_c}^2 t [1 + 8\bar{n}_c]) e^{-2i\omega_c t} \\ &\quad - \pi f(\omega_c) C_{\omega_c}^2 (2\bar{n}_c + 1) \frac{\sin(2\omega_c t)}{2\omega_c} \\ &= \left(\langle 0 | \hat{\rho}_d(t) | 2 \rangle \right)^*. \end{aligned} \quad (50)$$

These expressions reveal a qualitative difference compared with the case of a superposition confined to the lowest manifold $\{|0\rangle, |1\rangle\}$. In particular, even in the vacuum limit $\bar{n}_c = 0$, the matrix elements $\langle 2 | \hat{\rho}_d(t) | 2 \rangle$ and $\langle 0 | \hat{\rho}_d(t) | 2 \rangle$ decay irreversibly, indicating that this sector is not protected against gravitationally induced dissipation. The origin of this behavior lies in the quadratic detector-gravity coupling, which enforces a selection rule $\Delta n = \pm 2$ and therefore allows vacuum-fluctuation-induced transitions between $|2\rangle$ and $|0\rangle$ even when the gravitational field is in its ground state. By contrast, superpositions supported entirely within the $\{|0\rangle, |1\rangle\}$ manifold do not couple to the gravitational environment at leading order in the vacuum, so that no decoherence occurs at zero temperature.

At the same time, the ground-state population $\langle 0 | \hat{\rho}_d(t) | 0 \rangle$ increases linearly at short times. This increase does not signal a restoration of coherence or any violation of probability conservation. Rather, it reflects the redistribution of population within the truncated Hilbert space: transitions from $|2\rangle$ into $|0\rangle$ are permitted by the quadratic coupling, while the reverse process is absent in the vacuum because it would require absorption from an unoccupied gravitational mode. Consequently, population flows unidirectionally toward the ground state at zero temperature, producing the observed growth of $\langle 0 | \hat{\rho}_d(t) | 0 \rangle$. The trace of the density matrix remains conserved, and the reduced dynamics remains completely positive and trace preserving.

Such behavior is generic in open quantum systems: decay of coherence in one sector of Hilbert space is typically accompanied by population accumulation in another. What is specific to the present model is that this redistribution occurs only once the detector state involves levels separated by two quanta, consistent with the $\Delta n = \pm 2$ selection rule imposed by the quadratic detector-gravity interaction. In this sense, the $\{|0\rangle, |1\rangle\}$ manifold forms a protected subspace of the vacuum dynamics, whereas higher manifolds do not.

We observe that a thermal graviton state induces decoherence in the harmonic oscillator through genuine quantum fluctuations. To clarify the distinction between classical and quantum gravitational environments, we next model the gravitational field by a phase-randomized

coherent-state ensemble, which represents a classical stochastic background with identical average intensity but different fluctuation structure.

IV. CLASSICAL LIMIT OF GRAVITATIONAL DECOHERENCE

To isolate the effect of classical gravitational waves on the quantum detector, we model the gravitational field as a classical stochastic background represented by an ensemble of phase-randomized coherent states. As already emphasized at the beginning of the previous section, the gravitational field is quantized directly in the physical transverse-traceless sector. Consequently, the graviton creation and annihilation operators obey standard bosonic commutation relations,

$$[\hat{b}_k, \hat{b}_{k'}^\dagger] = \delta_{kk'}, \quad (51)$$

without the introduction of indefinite-metric structures or pseudo-commutators.

A multimode coherent state of the gravitational field is defined as a displaced vacuum [55, 56],

$$|\{\alpha_k\}\rangle = \hat{D}(\{\alpha_k\})|0\rangle_g; \quad \hat{D}(\{\alpha_k\}) = \exp\left(\sum_k \alpha_k \hat{b}_k^\dagger - \alpha_k^* \hat{b}_k\right), \quad (52)$$

where \hat{b}_k and \hat{b}_k^\dagger are the annihilation and creation operators of the physical plus polarized graviton mode k , $|0\rangle_g$ denotes the graviton vacuum, and $\alpha_k = |\alpha_k|e^{i\phi_k}$ specifies the amplitude and phase of each mode. Each mode satisfies $\hat{b}_k|\{\alpha_k\}\rangle = \alpha_k|\{\alpha_k\}\rangle$, so that the state factorizes as $|\{\alpha_k\}\rangle = \bigotimes_k |\alpha_k\rangle$.

The state of the gravitational sector is then taken to be

$$\rho_g^{\text{coh}} = \bigotimes_k \left(\int_0^{2\pi} \frac{d\phi_k}{2\pi} |\alpha_k\rangle\langle\alpha_k| \right), \quad (53)$$

where ρ_g^{coh} denotes the density matrix corresponding to coherent graviton states with randomized phases. The phases ϕ_k associated with different modes are assumed to be uncorrelated and uniformly distributed over the interval $[0, 2\pi)$.

The use of phase-randomized coherent states to represent a classical stochastic field has a long history in quantum field theory. In particular, it was shown in early studies of multiparticle production that a wide class of physically relevant density operators can be written in diagonal form in the coherent-state representation, with classical or chaotic sources corresponding to ensembles that are insensitive to the phases of the coherent amplitudes [55]. In such cases, one-point functions vanish while phase-invariant two-point correlators remain finite, capturing the statistical character of the underlying field. The phase averaging in Eq. (53) is therefore not

a dynamical assumption, but a minimal representation of an incoherent classical background.

A closely related phase-averaging mechanism appears in coherent states of charged bosons, where superselection rules enforce projection onto fixed-charge sectors and eliminate phase-sensitive observables [57]. In the present gravitational setting, however, the averaging reflects classical stochasticity rather than an exact symmetry constraint.

We emphasize that this construction also differs from early covariant coherent-state formulations of electromagnetism and linearized gravity based on indefinite-metric Hilbert spaces, where pseudo-commutation relations appear prior to the imposition of subsidiary conditions [58]. Here, the analysis is performed entirely within the physical graviton sector, and no pseudo-operator structures arise.

Physically, a pure coherent state corresponds to a deterministic classical gravitational wave (D1) with a well-defined amplitude and phase. The uniform phase averaging in Eq. (53) removes any global phase reference while preserving the classical energy content of each mode. As a result, the gravitational field is described as an incoherent classical background characterized by statistical properties rather than phase coherence. Such a phase-randomized coherent ensemble provides a minimal quantum representation of classical stochastic gravitational-wave backgrounds, as expected for radiation produced by many independent classical sources, such as unresolved astrophysical binaries or other incoherent emitters. In this case, the randomness originates from classical uncertainty in the phases rather than from intrinsic quantum fluctuations. Consequently, the gravitational field acts as a classical stochastic process rather than a quantum environment, even though it is conveniently represented using coherent states.

As a bookkeeping device for the classical limit, we distinguish the Planck constants in the gravitational and detector sectors by the substitutions $\hbar \rightarrow \hbar_G$ for gravitons, while $\hbar \rightarrow \hbar_D$ for the detector. This separation is introduced purely as a bookkeeping device to track the classical limit of the gravitational sector while keeping the detector fully quantum. Then in the interaction picture, and under the Born approximation, the reduced density matrix satisfies the second-order equation

$$\frac{d}{dt} \hat{\rho}_d(t) = -\frac{1}{\hbar_D^2} \int_0^\infty ds \text{Tr}_g \left[\hat{H}_{\text{int}}(t), [\hat{H}_{\text{int}}(t-s), \hat{\rho}_d(t) \otimes \rho_g] \right]. \quad (54)$$

Averaging over the coherent-state phases yields

$$\begin{aligned} \langle \hat{b}_l^\dagger \hat{b}_m^\dagger \rangle_g^\alpha &= 0, & \langle \hat{b}_l^\dagger \hat{b}_m \rangle_g^\alpha &= \delta_{lm} |\alpha_l|^2, \\ \langle \hat{b}_l \hat{b}_m^\dagger \rangle_g^\alpha &= \delta_{lm} (1 + |\alpha_l|^2), & \langle \hat{b}_l \hat{b}_m \rangle_g^\alpha &= 0, \\ \langle \hat{b}_l^\dagger \hat{b}_m^\dagger \rangle_g^{*\alpha} &= 0, & \langle \hat{b}_l^\dagger \hat{b}_m \rangle_g^{*\alpha} &= \delta_{lm} (1 + |\alpha_l|^2), \\ \langle \hat{b}_l \hat{b}_m^\dagger \rangle_g^{*\alpha} &= \delta_{lm} |\alpha_l|^2, & \langle \hat{b}_l \hat{b}_m \rangle_g^{*\alpha} &= 0, \end{aligned} \quad (55)$$

so that only the phase-neutral contributions survive. Proceeding exactly as in the fully quantum calculation,

the detector density matrix (33) evolves as

$$\begin{aligned} \hat{\rho}_d(t) = & e^{\hat{\mathcal{L}}_1 t} \hat{\rho}_d(0) e^{\hat{\mathcal{L}}_1 t} \\ & - \frac{\pi}{2} f(\omega_c) C_{\omega_c}^2 \int_0^t d\tau \left[(1 + |\alpha|^2) \right. \\ & \left. \mathcal{D}_+[\hat{\rho}_d(\tau)] + |\alpha|^2 \mathcal{D}_-[\hat{\rho}_d(\tau)] \right]. \end{aligned} \quad (56)$$

Here $|\alpha|^2 = |\alpha_k|^2|_{k=\omega_c}$ denotes the occupation number of the resonant gravitational-wave mode, and the dissipators \mathcal{D}_\pm are written explicitly following the same procedure as in Eq. (C3) of Appendix C, including the long-time averaging (although in the main text we presented the result without explicitly displaying this averaging step). The overall strength of the α -dependent dissipative contribution in Eq. (56) is governed by the effective rate

$$\Gamma_\alpha \equiv \pi f(\omega_c) C_{\omega_c}^2 |\alpha|^2, \quad (57)$$

which plays the role of a gravitationally induced damping (or decoherence) rate for the detector.

For the initial state given in Eq. (42), the density matrix elements evolve as

$$\langle 0 | \hat{\rho}_d(t) | 0 \rangle = \frac{1}{2} \left(1 - \frac{t}{\tau_\alpha} \right), \quad (58)$$

$$\langle 1 | \hat{\rho}_d(t) | 1 \rangle = \frac{1}{2} \left(1 - 3 \frac{t}{\tau_\alpha} \right), \quad (59)$$

$$\langle 0 | \hat{\rho}_d(t) | 1 \rangle = \frac{1}{2} \left(1 - 2 \frac{t}{\tau_\alpha} \right) e^{i\omega_c t}, \quad (60)$$

$$\langle 1 | \hat{\rho}_d(t) | 0 \rangle = \frac{1}{2} \left(1 - 2 \frac{t}{\tau_\alpha} \right) e^{-i\omega_c t}, \quad (61)$$

with the decoherence rate

$$\frac{1}{\tau_\alpha} = 2|\alpha|^2 \pi f(\omega_c) C_{\omega_c}^2. \quad (62)$$

The classical limit is implemented at the end of the calculation by scaling

$$C_{\omega_c} \sim \sqrt{\hbar_G}. \quad (63)$$

In the classical regime of the graviton sector, where the occupation number is large, $|\alpha_k|^2 \rightarrow \infty$, one has

$$\lim_{\substack{\hbar_G \rightarrow 0 \\ |\alpha|^2 \rightarrow \infty}} C_{\omega_c}^2 |\alpha|^2 \sim \text{constant}. \quad (64)$$

In this limit, the decoherence rate remains finite as $\hbar_G \rightarrow 0$, leading to a stochastic decoherence that is independent of temperature and vacuum fluctuations. Physically, this decoherence originates from the classical randomness of the gravitational field: each mode is represented by a coherent state with a fixed amplitude but a randomly distributed phase. It is worth emphasizing that this behavior is qualitatively distinct from that of a pure

coherent gravitational-wave state with a fixed phase. In that case, the α -dependent contributions to the reduced dynamics are purely oscillatory and, upon long-time (secular) averaging in the appropriate classical limit, the dissipative terms vanish identically. Consequently, the reduced evolution of the detector remains unitary and no decoherence is induced for any detector state. We refer the reader to Appendix D for a detailed demonstration.

Importantly, decoherence induced by a phase-randomized coherent background occurs irrespective of the initial state of the detector; even a detector prepared in a coherent superposition is not protected in the same way as the $\{|0\rangle, |1\rangle\}$ subspace. Consequently, decoherence generated by a classical, phase-randomized coherent state does not constitute direct evidence for the intrinsic quantum nature of gravitational waves. This behavior stands in sharp contrast to the fully quantum scenario, where a zero-temperature graviton environment does *not* induce decoherence.¹

V. THE DECOHERENCE TIME SCALE

In both the quantum and classical analyses, the decoherence rate is controlled by the spectral weight of the gravitational environment evaluated at the detector frequency together with the detector-bath coupling. From the perturbative master equation, the leading contribution to the decay of coherences is proportional to

$$\frac{1}{\tau_\alpha} \propto f(\omega_c) C_{\omega_c}^2, \quad (65)$$

where $f(\omega_c)$ denotes the density of graviton modes per unit frequency and C_{ω_c} is the mode-dependent coupling entering the interaction Hamiltonian.

From Eq. (16), the coupling coefficient is given by $C_\omega = \sqrt{\omega c \ell_p^2 / (2L^3)}$, and therefore scales as

$$C_\omega \propto \sqrt{\omega}. \quad (66)$$

Physically, this scaling reflects the fact that higher-frequency gravitational modes carry larger tidal gradients and therefore couple more strongly to the quadratic detector observable appearing in the interaction Hamiltonian. Substituting this into Eq. (65), we obtain the general scaling

$$\frac{1}{\tau_\alpha} \propto f(\omega_c) \omega_c. \quad (67)$$

¹ If the limit $\hbar_G \rightarrow 0$ is taken prematurely, the oscillatory structure of the interaction picture is lost, preventing the cancellation of intermediate \hbar_G factors. The classical limit must therefore be applied only after the full expression for the reduced dynamics has been obtained. In particular, taking $|\alpha_k| \rightarrow 0$ correctly reproduces the pure vacuum-induced dynamics discussed in the previous section.

This dependence on ω_c is physically natural: decoherence arises from energy- and phase-exchange processes between the detector mode and gravitational modes of comparable frequency. The available phase space for such processes is set by the density of graviton modes $f(\omega_c)$, while the interaction strength contributes the additional factor of ω_c .

To make the discussion concrete, let us consider a general power-law form for the gravitational spectral density,

$$f(\omega) \propto \omega^s, \quad (68)$$

which yields

$$\frac{1}{\tau_\alpha} \propto \omega_c^{s+1}. \quad (69)$$

Different values of the exponent α lead to qualitatively different behaviour:

- For $s = -1$, the decoherence rate is independent of the detector frequency, $\tau_\alpha^{-1} = \text{const}$, as shown by the green curve in Fig. 1.
- For $s > -1$, the decoherence rate increases with ω_c , illustrated by the blue curve ($s = 1$).
- For $s < -1$, the decoherence rate decreases with increasing ω_c , as shown by the yellow curve ($s = -2$).

For free gravitons propagating in 3+1 dimensions, the spectral density follows from the density of states of a massless field. Since $\omega = c|\mathbf{k}|$, the number of modes in a shell $k \rightarrow k + dk$ scales as $4\pi k^2 dk$, implying

$$f(\omega) \propto \omega^2. \quad (70)$$

This implies that, all else being equal, higher-frequency detectors experience stronger gravitationally induced decoherence. In practice, however, this advantage is counterbalanced by experimental constraints such as increased thermal noise, reduced coherence times, and limitations in state preparation and readout at high frequencies.

More importantly, Eq. (67) underscores a key conceptual point: the decoherence time cannot be predicted independently without specifying the spectral profile of the gravitational environment. Since $f(\omega)$ depends on the astrophysical or cosmological origin of the gravitational background, the same detector may experience vastly different decoherence rates in different gravitational settings. Moreover, the ultimate manifestation of gravitationally induced decoherence depends not only on the spectral structure of the environment but also on the quantum state of the gravitons and on the initially prepared state of the detector system.

This observation reinforces the central theme of the present work—it is the structure and selectivity of decoherence, rather than its absolute magnitude, that encodes information about the underlying gravitational background.

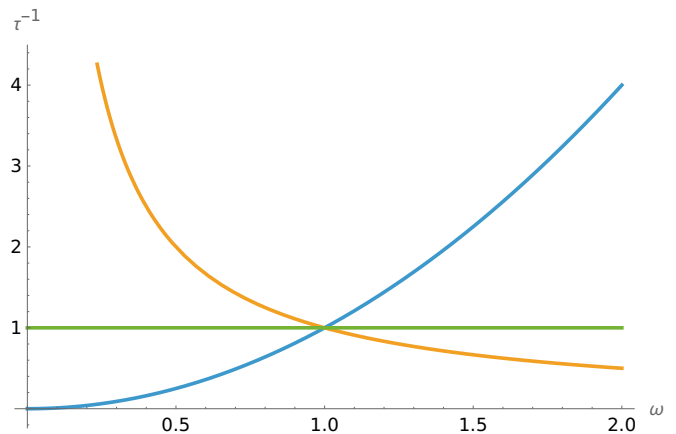


Figure 1. Inverse decoherence time τ_α^{-1} as a function of the detector frequency ω_c for different spectral profiles $f(\omega_c) \propto \omega_c^s$. The green, blue, and yellow curves correspond respectively to $s = -1, 1$, and -2 , illustrating the strong sensitivity of the decoherence rate to the gravitational spectral density.

VI. EXPERIMENTAL PROTOCOL: STATE-SELECTIVE TEST OF GRAVITATIONAL DECOHERENCE

The results obtained in this work suggest a conceptually robust strategy for probing the microscopic nature of gravitational waves using quantum-controlled mechanical systems. A central outcome of our analysis is that the structure of gravitationally induced decoherence—rather than its absolute magnitude—provides the relevant experimental diagnostic. In particular, the perturbative master equation derived in Sec. III [see Eq. (32)] predicts a qualitatively different response of low-lying Fock manifolds depending on whether the gravitational background is a quantum vacuum or a classical stochastic field.

This distinction follows directly from the explicit solutions of the reduced dynamics. For vacuum gravitons, the quadratic detector-gravity coupling imposes selection rules that suppress all leading-order dissipative contributions within the lowest Fock manifold $\{|0\rangle, |1\rangle\}$ [see Eq. (45)]. As a result, coherent superpositions supported entirely within this subspace do not decohere at zero temperature in the absence of other environments. By contrast, classical stochastic gravitational-wave backgrounds—including phase-randomized coherent states and thermal graviton ensembles—produce finite decoherence rates already in the lowest Fock sector. This qualitative difference motivates the state-selective experimental protocol outlined below.

Crucially, however, the absence of observable decoherence in the $\{|0\rangle, |1\rangle\}$ subspace cannot by itself establish the quantum nature of gravity, since unavoidable environmental channels will always contribute residual damping and dephasing. The discriminatory power of our proposal instead lies in a comparative, state-selective strategy that exploits the different scaling of decoherence across

Fock manifolds.

Step 1: Preparation of low-lying phonon superpositions

Consider a single mechanical mode whose phonon states can be prepared and measured with high fidelity. Modern hybrid quantum platforms—including GHz-frequency bulk-acoustic-wave resonators, membrane-in-the-middle systems, and optomechanical crystal cavities coupled to superconducting qubits—permit deterministic preparation of low-lying phonon number states and their coherent superpositions via qubit–mechanical or optical state-transfer protocols [59–61].

Under otherwise identical experimental conditions, prepare the two initial states

$$|\psi_{01}\rangle = \frac{1}{\sqrt{2}}(|0\rangle + |1\rangle), \quad |\psi_{02}\rangle = \frac{1}{\sqrt{2}}(|0\rangle + |2\rangle). \quad (71)$$

Step 2: Measurement of relaxation and coherence times

A first experimental probe consists of preparing the mechanical mode in the state $|1\rangle$, allowing it to evolve freely, and measuring the population $\langle 1|\rho_d(t)|1\rangle$ as a function of time. The observed decay defines an effective relaxation time T_1 , which at short times is well described by a single exponential,

$$T_1^{-1} = \gamma + \Gamma_{11}^{\text{grav}}, \quad (72)$$

where γ denotes the intrinsic (non-gravitational) mechanical damping rate, and $\Gamma_{11}^{\text{grav}} = 3/\tau_G$ is the gravitationally induced contribution, as obtained from Eq. (C16).

An independent probe is obtained by preparing the coherent superposition $(|0\rangle + |1\rangle)/\sqrt{2}$ and performing a phase-sensitive Ramsey-type measurement [59, 60] to monitor the decay of the off-diagonal density matrix element $\langle 0|\rho_d(t)|1\rangle$. The decay of the Ramsey fringe envelope defines an effective coherence time T_2 , which at short times obeys

$$T_2^{-1} = \frac{\gamma}{2} + \Gamma_{01}^{\text{grav}}, \quad (73)$$

where $\Gamma_{01}^{\text{grav}} = 2/\tau_G$ follows from Eq. (C19).

Both T_1 and T_2 are therefore experimentally accessible observables characterizing decoherence within the lowest Fock manifold. Importantly, neither quantity alone suffices to disentangle gravitationally induced decoherence from ordinary environmental noise, motivating the comparative strategy described below.

Step 3: Gravitational decoherence rates from theory

From the perturbative solution of the master equation, the gravitationally induced decoherence rates for a ther-

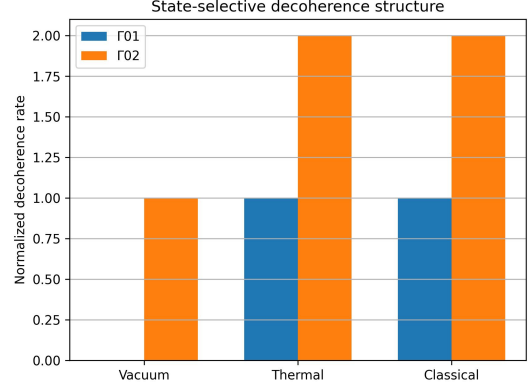


Figure 2. Comparison of gravitationally induced decoherence rates for the lowest Fock superpositions. In a quantum-vacuum gravitational environment the rate Γ_{01} vanishes while Γ_{02} remains finite, reflecting the $\Delta n = \pm 2$ selection rule of the quadratic coupling. Thermal and classical phase-randomized gravitational backgrounds instead exhibit the universal scaling $\Gamma_{02} = 2\Gamma_{01}$, indicating the absence of a protected subspace.

mal graviton environment with mean occupation number \bar{n}_c are obtained as

$$\Gamma_{01}^{\text{grav,th}} = 4\pi \bar{n}_c f(\omega_c) C_{\omega_c}^2, \quad (74)$$

$$\Gamma_{11}^{\text{grav,th}} = 6\pi \bar{n}_c f(\omega_c) C_{\omega_c}^2, \quad (75)$$

as follows from Eq. (40). For superpositions involving the second excited state one similarly finds

$$\Gamma_{02}^{\text{grav,th}} = \pi f(\omega_c) C_{\omega_c}^2 (1 + 8\bar{n}_c), \quad (76)$$

$$\Gamma_{22}^{\text{grav,th}} = 2\pi f(\omega_c) C_{\omega_c}^2 (1 + 6\bar{n}_c), \quad (77)$$

as obtained from Eq. (50).

Taking the vacuum limit $\bar{n}_c \rightarrow 0$ yields the key structural result

$$\Gamma_{01}^{\text{grav,vac}} = 0, \quad \Gamma_{02}^{\text{grav,vac}} = \pi f(\omega_c) C_{\omega_c}^2 \neq 0. \quad (78)$$

Thus, at leading order the vacuum gravitational environment does not induce decoherence for superpositions supported entirely within the $\{|0\rangle, |1\rangle\}$ manifold, while decoherence appears once states separated by two quanta are involved. This behavior follows directly from the quadratic detector–gravity coupling, which enforces the selection rule $\Delta n = \pm 2$.

By contrast, thermal graviton states and classical stochastic gravitational backgrounds generate decoherence already in the lowest Fock manifold and obey the universal scaling $\Gamma_{02} = 2\Gamma_{01}$ at small occupation numbers. The resulting structural difference between the vacuum and stochastic cases is illustrated in Fig. 2, which compares the rates Γ_{01} and Γ_{02} across the different gravitational environments.

Step 4: Construction of a dimensionless selectivity ratio

Because gravitational decoherence cannot be isolated from environmental noise at the level of absolute rates, we introduce a dimensionless observable that depends only on the *relative scaling* of decoherence across Fock manifolds:

$$R \equiv \frac{\Gamma_{02}^{\text{tot}}}{2\Gamma_{01}^{\text{tot}}}, \quad (79)$$

where $\Gamma_{ij}^{\text{tot}} = \Gamma_{ij}^{\text{env}} + \Gamma_{ij}^{\text{grav}}$ are the experimentally measured total decoherence rates. For generic Markovian non-gravitational environments described by Lindblad operators that are linear in the oscillator variables, the decoherence rates exhibit a universal scaling, $\Gamma_{n_1 n_2}^{\text{env}} \propto n_1 + n_2$ (see Eq. (C8)). As a result, $\Gamma_{02}^{\text{env}} = 2\Gamma_{01}^{\text{env}}$, yielding $R = 1$ independently of the microscopic details of the environment.

Importantly, this behavior is both qualitatively and quantitatively identical to that obtained for thermal graviton backgrounds and for phase-randomized coherent gravitational states in the regime of sufficiently large occupation numbers. Although these two states represent distinct physical descriptions — a mixed quantum Gaussian state and a classical stochastic ensemble, respectively — they yield identical second-order correlation functions at the detector frequency. Consequently, the induced decoherence rates obey the universal scaling

$$\Gamma_{02}^{\text{grav}} \simeq 2\Gamma_{01}^{\text{grav}}, \quad (80)$$

with the overall magnitude controlled by the occupation number of the background: \bar{n}_c for a thermal state and $|\alpha|^2$ for a phase-randomized coherent state. Indeed, the latter case can be obtained from the former by the formal replacement $\bar{n}_c \rightarrow |\alpha|^2$, as follows from Eq. (62).

Step 5: Interpretation and no-go criterion

The experimentally measured ratio

$$R \equiv \frac{\Gamma_{02}}{2\Gamma_{01}} \quad (81)$$

provides a state-selective diagnostic of the gravitational environment. Its interpretation is summarized in Fig. 3 and can be stated as follows:

- $R \simeq 1$: consistent with ordinary environmental decoherence, classical stochastic gravitational-wave backgrounds, thermal graviton states, or phase-randomized coherent gravitational radiation. In all these cases the decoherence rates obey the universal scaling $\Gamma_{02} = 2\Gamma_{01}$, so that no protected subspace exists in the lowest Fock manifold.

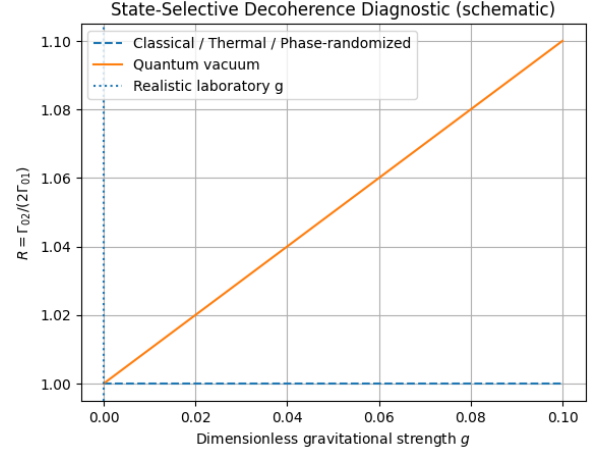


Figure 3. Schematic illustration of the state-selective diagnostic. Classical stochastic, thermal, and phase-randomized coherent gravitational backgrounds yield the universal scaling $\Gamma_{02} = 2\Gamma_{01}$ and therefore $R = 1$. Vacuum fluctuations of a quantized gravitational field instead produce $R = 1 + g$, reflecting suppression of decoherence within the $\{|0\rangle, |1\rangle\}$ manifold. The horizontal axis is displayed schematically for clarity; realistic laboratory parameters correspond to $g \ll 1$.

- $R > 1$: indicates suppression of decoherence within the $\{|0\rangle, |1\rangle\}$ manifold while decoherence persists for superpositions involving higher Fock states. This behavior arises from the quadratic detector-gravity coupling and is uniquely consistent, at leading order, with vacuum fluctuations of a quantized gravitational field.

To make this statement explicit, consider a quantum gravitational vacuum in the presence of a generic Markovian environment. The total decoherence rates can be written as

$$\Gamma_{01}^{\text{tot}} = \Gamma_{01}^{\text{env}}, \quad \Gamma_{02}^{\text{tot}} = \Gamma_{02}^{\text{env}} + \Gamma_{02}^{\text{grav}}, \quad (82)$$

where the vacuum graviton contribution satisfies $\Gamma_{01}^{\text{grav}} = 0$ and $\Gamma_{02}^{\text{grav}} \neq 0$. For standard environmental channels described by operators linear in the oscillator variables one has $\Gamma_{02}^{\text{env}} = 2\Gamma_{01}^{\text{env}}$, yielding

$$R = \frac{\Gamma_{02}^{\text{tot}}}{2\Gamma_{01}^{\text{tot}}} = 1 + \frac{\Gamma_{02}^{\text{grav}}}{2\Gamma_{01}^{\text{env}}} > 1. \quad (83)$$

Any statistically significant deviation of R from unity therefore signals a structural suppression of decoherence in the lowest Fock manifold. Such a deviation cannot be reproduced by classical stochastic gravitational-wave backgrounds, thermal graviton states, or phase-randomized coherent radiation derived from the same microscopic coupling. Within the perturbative regime considered here, it constitutes an operational signature consistent only with vacuum fluctuations of a quantized gravitational field.

Feasibility and outlook

The absolute magnitude of gravitationally induced decoherence predicted by the present framework is strongly suppressed by the Planck scale. In a quantum-vacuum gravitational environment, the leading nonvanishing contribution arises only for superpositions differing by two quanta and is parametrically proportional to $f(\omega_c)C_{\omega_c}^2 \sim G\omega_c^5$. The corresponding decoherence times therefore exceed present mechanical coherence times by many orders of magnitude, making direct observation of vacuum graviton emission in mesoscopic systems unrealistic in the near term.

The experimentally relevant question is instead whether non-vacuum gravitational backgrounds contribute measurable decoherence beyond well-characterized environmental channels. The detector frequency considered here lies in the GHz regime, corresponding to the operational band of current high-frequency mechanical resonators such as HBAR devices. Standard slow-roll inflation produces a squeezed vacuum spectrum of tensor modes whose present-day frequencies typically do not extend far beyond $\mathcal{O}(10^7 \text{ Hz})$ after cosmological redshift [62]. Thus conventional inflationary vacuum fluctuations do not naturally populate the GHz band [63]. Any nonzero occupation number at GHz frequencies must therefore originate from alternative high-frequency production mechanisms [64], such as post-inflationary preheating dynamics, high-scale phase transitions, compact sources (e.g. primordial black hole binaries), or other exotic gravitational processes [65–67]. Our analysis does not assume any specific cosmological origin and constrains only the occupation number at the detector frequency.

For thermal or phase-randomized coherent graviton states, the decoherence rate scales linearly with the mean occupation number \bar{n}_c (or $|\alpha|^2$). Using the continuum spectral density $f(\omega_c) = \omega_c^2$ and the coupling $C_{\omega_c}^2 = \omega_c \hbar G / (2c^2)$, the gravitational contribution to the lowest-manifold decoherence rate becomes

$$\Gamma_{01}^{\text{grav}} = \frac{\hbar G}{\pi c^2} \omega_c^3 \bar{n}_c. \quad (84)$$

For an HBAR device with $\omega_c = 2\pi \times 5.96 \text{ GHz}$ [30, 31], this evaluates numerically to

$$\Gamma_{01}^{\text{grav}} \approx 1.3 \times 10^{-30} \bar{n}_c \text{ s}^{-1}. \quad (85)$$

Demanding that no anomalous decoherence exceed the measured mechanical dephasing rate $\Gamma_{\text{env}} \sim 10^4 \text{ s}^{-1}$ implies the bound

$$\bar{n}_c \lesssim 8 \times 10^{33}. \quad (86)$$

Thus present GHz mechanical experiments already constrain non-vacuum gravitational radiation backgrounds to have effective occupation numbers below $\sim 10^{34}$ near ω_c . Although numerically large, this bound directly reflects the Planck suppression of the gravitational coupling

at GHz frequencies and is independent of cosmological model assumptions within the perturbative regime considered here.

Complementary information is obtained from the state-selective ratio $R = \Gamma_{02}/(2\Gamma_{01})$. Thermal graviton states, classical stochastic backgrounds, and phase-randomized coherent states all obey the universal scaling $\Gamma_{02} = 2\Gamma_{01}$, implying

$$R = 1. \quad (87)$$

If an experiment verifies $|R - 1| < \varepsilon$ within statistical precision ε , any vacuum-induced contribution must satisfy

$$\Gamma_{02}^{\text{grav,vac}} < 2\varepsilon \Gamma_{01}^{\text{env}}. \quad (88)$$

Conversely, a statistically significant deviation of R from unity would indicate suppression of decoherence within the $\{|0\rangle, |1\rangle\}$ manifold and cannot be reproduced by classical or stochastic gravitational backgrounds derived from the same microscopic coupling. Within the perturbative regime, such a deviation would therefore be consistent only with vacuum-induced two-quantum processes.

The protocol thus provides two independent constraints: (i) an absolute-rate bound on non-vacuum graviton occupation, and (ii) a structural bound on vacuum-induced decoherence derived from deviations of R from unity. Improvements in mechanical coherence time, state-preparation fidelity, and statistical precision translate directly into progressively stronger bounds on both quantities.

While Planck-suppressed vacuum effects remain far below current experimental sensitivity, continued advances in cryogenic optomechanics [68], circuit quantum acoustodynamics [69], and high-overtone bulk acoustic resonator [30] platforms steadily extend coherence times and quantum control capabilities. Within this trajectory, the framework developed here provides a concrete operational roadmap for constraining the quantum state of gravitational radiation using mesoscopic quantum systems.

VII. CONCLUSION

In this work we have developed a unified and internally consistent framework for analysing how gravitational waves—treated either as a quantized field or as a classical stochastic background—affect the coherence properties of a mesoscopic quantum system. Starting from a common microscopic coupling between a harmonic oscillator and a weak gravitational perturbation, we derived the reduced dynamics in both the quantum and classical descriptions and compared the resulting master equations on equal footing. This unified treatment eliminates model-dependent assumptions and makes the dynamical differences between distinct gravitational environments directly visible at the level of observable decoherence.

Environment	Physical interpretation	Decoherence?	Protected?
Pure coherent state (fixed phase)	Deterministic classical gravitational wave	No	N/A
Phase-randomized coherent ensemble	Classical stochastic gravitational-wave background	Yes	No
Thermal graviton state	Gaussian state (parametrization of non-vacuum quantum backgrounds)	Yes	No
Quantum vacuum	Quantum vacuum fluctuations of the gravitational field	Selective	Yes

Table I. Classification of gravitational environments analyzed in this work. Only the vacuum state leads to a protected low-phonon manifold at leading order.

Our central finding is that *decoherence by itself is not a signature of quantum gravity*. Classical stochastic gravitational-wave backgrounds, quantum thermal graviton fields, and quantum vacuum fluctuations can all induce decoherence in an open quantum system. What distinguishes these scenarios is instead the *structure* of the induced reduced dynamics. In particular, in the quantum-vacuum case decoherence arises solely through spontaneous emission of real, on-shell gravitons, leading to a two-quantum selection rule that suppresses transitions within the lowest-excitation manifold $\{|0\rangle, |1\rangle\}$ at leading order. By contrast, a classical stochastic gravitational background generically induces phase diffusion even within this same subspace, thereby removing the protection.

This structural distinction provides a sharp operational criterion (see Table I). The absence of decoherence in the $\{|0\rangle, |1\rangle\}$ manifold is consistent only with a quantum gravitational vacuum, whereas the observation of decoherence within this nominally protected sector would rule out a purely vacuum description of the gravitational field, independently of the absolute magnitude of the decoherence rate. Deterministic classical gravitational waves—described by coherent states of the field—produce unitary dynamics without intrinsic decoherence, highlighting that stochasticity rather than classicality per se is the essential ingredient behind classical gravitational decoherence.

At the level of linearized quantum field theory there exists a single dynamical gravitational field $h_{\mu\nu}$, and the distinction between “external” and “self” gravity is not fundamental. Static gravitational interactions arise from virtual graviton exchange at tree level and correspond to conservative forces such as the Newtonian potential, while gravitational radiation corresponds to the emission of real, on-shell gravitons. The vacuum state is simply the ground state of this field. Consequently, whether gravity acts as an external environment or as a channel for spontaneous emission is determined by the quantum state in which the field is prepared, rather than by a structural difference in the interaction itself.

In the vacuum setting, coherence protection within $\{|0\rangle, |1\rangle\}$ follows from the two-quantum transition mechanism associated with spontaneous graviton radiation, as shown in quantum-field-theoretic analyses of harmonic systems [70]. Our contribution is to demonstrate that this protection is not a universal consequence of weak gravitational coupling, but a property specific to the vacuum state of the gravitational field. When the same mi-

croscopic coupling is considered for classical stochastic or non-vacuum gravitational configurations, the protected subspace generically disappears. In this way, coherence protection is elevated from a radiation-theory result to a structural diagnostic of gravitational ‘quantum’-ness.

We emphasize that the Born–Markov treatment adopted here does not exclude spontaneous graviton emission by the detector [71]. Consistency requires only that the detector-induced modification of the gravitational bath remain perturbatively small. As shown in Appendix E, the emission rate is suppressed by the Planck scale, leading to an occupation number $\langle b_k^\dagger b_k \rangle \sim \gamma_{\text{em}} t \ll 1$ over experimentally relevant timescales. The gravitational bath therefore remains effectively in its initial state to leading order, ensuring that the factorization assumption underlying the master-equation derivation is self-consistent.

Quantitatively, present GHz mechanical experiments already constrain non-vacuum gravitational radiation backgrounds in the quantum regime. Using experimentally accessible parameters for high-overtone bulk acoustic resonators, the absence of excess decoherence beyond measured environmental dephasing implies an upper bound on the effective graviton occupation number at GHz frequencies of order $\bar{n}_c \lesssim 10^{34}$. Although numerically large, this bound directly reflects the extreme Planck suppression of gravitational couplings at these frequencies and constitutes a direct quantum-regime constraint on non-vacuum gravitational backgrounds within the perturbative framework considered here.

Complementary information is obtained from the state-selective ratio $R = \Gamma_{02}/(2\Gamma_{01})$. Thermal graviton states, classical stochastic backgrounds, and phase-randomized coherent states all yield the universal scaling $\Gamma_{02} = 2\Gamma_{01}$ and therefore $R = 1$. If an experiment were to observe a statistically significant deviation $|R - 1| > \varepsilon$, such a deviation could not be reproduced by these non-vacuum gravitational configurations derived from the same microscopic interaction and would instead indicate vacuum-induced two-quantum processes at leading order. In this sense, improvements in coherence time and statistical precision translate directly into progressively tighter bounds on both non-vacuum gravitational occupation and vacuum-induced decoherence contributions.

Conceptually, the present work shifts the focus of gravitational decoherence studies from the magnitude of decay rates to the qualitative structure of reduced dynam-

ics. Rather than asking whether gravity induces decoherence, we ask how the pattern of decoherence depends on the microscopic state of the gravitational field. This reframing provides a clear and experimentally falsifiable criterion rooted in symmetry and selection rules rather than absolute rate estimates.

An interesting extension of the present framework would be to analyze gravitational environments prepared in squeezed quantum states. Time-dependent gravitational backgrounds, such as cosmological expansion or dynamical matter sources, are known to generically generate squeezed states of graviton modes in perturbative quantum gravity [72]. Since squeezed states introduce additional anomalous correlations in the environmental two-point functions, incorporating such gravitational environments within the open-system treatment developed here could modify the structure of the induced master equation and potentially lead to new signatures in the decoherence pattern of mesoscopic quantum probes. Exploring these effects would provide a natural generalization of the present analysis and further clarify how different quantum states of gravitational radiation are reflected in detector dynamics.

Experimentally, quantum systems are inevitably open, and environmental decoherence from electromagnetic, thermal, and material noise cannot be fully eliminated. However, advances in cryogenic optomechanics, circuit-mechanical architectures, and high-overtone bulk acoustic resonators (HBARs) coupled to superconducting qubits already enable preparation of lowest-excitation states, including coherent superpositions of $|0\rangle$ and $|1\rangle$, as well as nonclassical mechanical states. The state family required for the present proposal is therefore technologically accessible, independent of the specific hardware implementation. While current coherence times remain insufficient to observe Planck-suppressed vacuum effects directly, the identification of protected and unprotected manifolds enables differential measurements robust against unknown environmental noise. Within this trajectory, the framework developed here establishes a concrete operational roadmap for probing and constraining the microscopic quantum state of gravitational radiation using mesoscopic quantum systems.

In summary, while decoherence is a generic feature of open quantum systems, its *state-dependent structure* can serve as an operational probe of the microscopic nature of gravitational radiation. The persistence or breakdown of coherence within the lowest-excitation manifold provides a precise and experimentally meaningful discriminator between a quantum gravitational vacuum and classical or stochastic gravitational backgrounds. This state-selective approach offers a conceptually distinct route to probing the quantumness of gravity—one rooted not in the magnitude of energy exchange, but in the qualitative structure of quantum coherence.

ACKNOWLEDGMENTS

P.N. acknowledges support from the National Institute for Theoretical and Computational Sciences (NITheCS) through the Rector's Postdoctoral Fellowship Programme (RFPF). He thanks Prof. Douglas Singleton and Prof. Kazuhiro Yamamoto for their helpful comments and keen interest in this work.

P.N. and S.S. also thanks Dr. Sandro Donadi and Dr. Matteo Fadel for useful discussions and correspondence. P.N. is grateful to Prof. Ananda Das Gupta and Prof. Golam Mortuza Hossain for constructive comments on the Born–Markov approximation and for arranging an invited lecture at the Indian Institute of Science Education and Research (IISER) Kolkata.

Appendix A: Derivation of the Hamiltonian for graviton modes

The analysis is being followed from [22, 23] We start from linearized gravity about Minkowski space,

$$g_{\mu\nu} = \eta_{\mu\nu} + h_{\mu\nu}, \quad |h_{\mu\nu}| \ll 1, \quad (\text{A1})$$

and impose the transverse–traceless (TT) gauge on the spatial components:

$$h_{0\mu} = 0, \quad \partial^i h_{ij} = 0, \quad h^i{}_i = 0. \quad (\text{A2})$$

In this gauge the quadratic (free) gravitational (Einstein–Hilbert) action is

$$\begin{aligned} S_{\text{grav}} &= -\frac{1}{64\pi G} \int d^4x (\partial_\alpha h_{ij})(\partial^\alpha h^{ij}) \\ &= \frac{1}{64\pi G} \int d^4x (\dot{h}_{ij}\dot{h}^{ij} - \partial_k h_{ij} \partial_k h^{ij}). \end{aligned} \quad (\text{A3})$$

To exhibit the canonical variables, we decompose the metric deformation into TT plane waves in a cubic box of side L (volume $V = L^3$):

$$h_{ij}(t, \vec{x}) = \frac{1}{\sqrt{\hbar G}} \sum_{\vec{k}, s=\{+, \times\}} q_{\vec{k}, s}(t) e^{i\vec{k}\cdot\vec{x}} \epsilon_{ij}^{(s)}(\vec{k}), \quad (\text{A4})$$

where $\epsilon_{ij}^{(s)}(\vec{k})$ are real, transverse and traceless polarization tensors, orthonormal on the TT subspace. The “canonical coordinate” for each graviton degree of freedom is the TT-projected Fourier amplitude of the metric deformation:

$$q_{\vec{k}, s}(t) = \sqrt{\hbar G} \frac{1}{V} \int d^3x e^{-i\vec{k}\cdot\vec{x}} \epsilon_{ij}^{(s)}(\vec{k}) h_{ij}(t, \vec{x}), \quad (\text{A5})$$

so that the metric perturbation is reconstructed from the set $\{q_{\vec{k}, s}\}$ by the inverse expansion above. Reality of h_{ij} implies $q_{\vec{k}, s}^*(t) \epsilon_{ij}^{(s)}(\vec{k}) = q_{-\vec{k}, s}(t) \epsilon_{ij}^{(s)}(-\vec{k})$.

Substituting the mode expansion and using $\int_V d^3x e^{i(\vec{k}-\vec{k}')\cdot\vec{x}} = V \delta_{\vec{k},\vec{k}'}$ and polarization orthonormality, the action becomes a sum of decoupled oscillators:

$$S = \frac{L^3}{32\pi \hbar G^2} \int dt \sum_{\vec{k},s} \left(\dot{q}_{\vec{k},s}^2 - \omega_k^2 q_{\vec{k},s}^2 \right) \equiv \int dt \mathcal{L}, \quad \omega_k \equiv |\vec{k}|. \quad (\text{A6})$$

Here L denotes the linear size of the normalization volume $V = L^3$ introduced in the canonical quantization procedure. In the continuum limit, the explicit dependence on L cancels against the density of states. For a gravitational mode of frequency ω_g (setting $c = 1$), the physically relevant scale governing the interaction is the corresponding wavelength $\lambda_g \sim 1/\omega_g$.

The canonical momentum conjugate to $q_{\vec{k},s}$ is

$$p_{\vec{k},s} \equiv \frac{\partial \mathcal{L}}{\partial \dot{q}_{\vec{k},s}} = \frac{L^3}{16\pi \hbar G^2} \dot{q}_{\vec{k},s}, \quad (\text{A7})$$

so that

$$\dot{q}_{\vec{k},s} = \frac{16\pi \hbar G^2}{L^3} p_{\vec{k},s}, \quad (\text{A8})$$

$$p_{\vec{k},s} = \frac{L^3}{16\pi \hbar G^2} \dot{q}_{\vec{k},s}. \quad (\text{A9})$$

It is now convenient to introduce a mode-independent ‘‘mass’’ parameter

$$m \equiv \frac{L^3}{16\pi \hbar G^2}, \quad (\text{A10})$$

so that the Hamiltonian for each mode takes the standard harmonic-oscillator form:

$$H_{\vec{k},s} = \frac{p_{\vec{k},s}^2}{2m} + \frac{1}{2} m \omega_k^2 q_{\vec{k},s}^2, \quad H = \sum_{\vec{k},s} H_{\vec{k},s}. \quad (\text{A11})$$

For concreteness, let us focus on a single mode with wave vector along the $+\hat{z}$ direction and frequency

$$\omega_k = \omega_k^g = |\vec{k}|, \quad (\text{A12})$$

restricted to the $+$ polarization for simplicity (the \times polarization being dynamically identical at the free-field level). In this case, the effective action and Hamiltonian reduce to The action and Hamiltonian for a single graviton mode are

$$S_{\omega_g} = \int dt \frac{1}{2} m (\dot{q}_+^2 - (\omega_k^g)^2 q_+^2), \quad (\text{A13})$$

$$H_{\omega_g} = \frac{p_+^2}{2m} + \frac{1}{2} m (\omega_k^g)^2 q_+^2. \quad (\text{A14})$$

where q_+ and p_+ are the canonical coordinate and momentum of the graviton mode with frequency ω_k^g and effective mass m .

where, for brevity, we have denoted $q_{\vec{k},+} \rightarrow q_+$ and $p_{\vec{k},+} \rightarrow p_+$. Canonical quantization promotes (q_+, p_+)

to operators with $[\hat{q}_+, \hat{p}_+] = i\hbar$. Introducing the ladder operators

$$\begin{aligned} \hat{b}_k &= \sqrt{\frac{m \omega_k^g}{2\hbar}} \hat{q}_+ + \frac{i}{\sqrt{2m\hbar\omega_k^g}} \hat{p}_+, \\ \hat{b}_k^\dagger &= \sqrt{\frac{m \omega_k^g}{2\hbar}} \hat{q}_+ - \frac{i}{\sqrt{2m\hbar\omega_k^g}} \hat{p}_+. \end{aligned} \quad (\text{A15})$$

which satisfy $[\hat{b}_k, \hat{b}_k^\dagger] = 1$, the Hamiltonian for a single graviton mode can be expressed in normal-ordered form as

$$\hat{H}_G \equiv \hat{H}_{\omega_k^g} = \hbar\omega_k^g : \hat{b}_k^\dagger \hat{b}_k :, \quad (\text{A16})$$

where the colons denote normal ordering, ensuring that the vacuum contribution is omitted. Each transverse-traceless (TT) graviton mode (\vec{k}, s) thus corresponds to a quantum harmonic oscillator of frequency $\omega_g = |\vec{k}|$, with canonical coordinate given by the TT-projected Fourier amplitude of the metric perturbation, and canonical momentum proportional to its time derivative, as defined above.

As we have chosen only the plus polarization for the GW, for each mode of the GW i.e. for each \vec{k} , we can have

$$h_{ij}(t) = 2\chi(t)\epsilon_+ \sigma_{ij}^3 = \frac{1}{\sqrt{\hbar G}} q_+(t) e^{i\vec{k}\cdot\vec{x}} \epsilon_{ij}^+(\vec{k}), \quad (\text{A17})$$

where $\epsilon_{ij}^+(\vec{k})$ is the polarization tensor corresponding to the plus polarization. Then from (A17), we get

$$\chi(t) = \frac{1}{2\sqrt{\hbar G}} q_+(t) e^{i\vec{k}\cdot\vec{x}}, \quad (\text{A18})$$

which for GWs moving along z-direction reduces to $\chi(t) = \frac{1}{2\sqrt{\hbar G}} q_+(t) e^{ikz}$. Again, we have already promoted $q_+ \rightarrow \hat{q}_+$ i.e to its quantum status. Then, we can expand \hat{q}_+ in terms of its modes as: $\hat{q}_+ = \sqrt{\frac{\hbar}{2m\omega_g}} (\hat{b}_g e^{-i\omega_g t} + \hat{b}_g^\dagger e^{i\omega_g t})$. Then, elevating $\chi(t)$ to its corresponding operator and without loss of generality choosing $z = 0$, we get

$$\hat{\chi}(t) = \frac{1}{2\sqrt{\hbar G}} \sqrt{\frac{\hbar}{2m\omega_g}} (\hat{b}_g e^{-i\omega_g t} + \hat{b}_g^\dagger e^{i\omega_g t}). \quad (\text{A19})$$

This will yield (16).

Appendix B: Computation of Eq (29)

In this appendix, we derive the terms appearing in Eq. (29).

Starting from the interaction Hamiltonian, we have

$$\begin{aligned}
& \int_0^\infty ds \langle \hat{H}_{\text{int}}(t) \hat{H}_{\text{int}}(t-s) \hat{\rho}_d(t) \rangle_g \\
&= \hbar^2 \int_0^\infty ds \sum_{l,m} \mathcal{C}_{\omega_l^g} \mathcal{C}_{\omega_m^g} \left\langle \left[\hat{b}_l \hat{a}_1^{\dagger 2} e^{i(2\omega_c - 2\omega_l^g)t} \right. \right. \\
&\quad \left. \left. - \hat{b}_l \hat{a}_1^2 e^{-i(2\omega_c + 2\omega_l^g)t} \right. \right. \\
&\quad \left. \left. + \text{h.c.} \right] \right. \\
&\quad \left. \times \left[\hat{b}_m \hat{a}_1^{\dagger 2} e^{i(2\omega_c - 2\omega_m^g)(t-s)} - \hat{b}_m \hat{a}_1^2 e^{-i(2\omega_c + 2\omega_m^g)(t-s)} + \text{h.c.} \right] \right. \\
&\quad \left. \hat{\rho}_d(t) \right\rangle_g. \tag{B1}
\end{aligned}$$

Evaluating the expectation values and keeping only non-vanishing contributions, we obtain

$$\begin{aligned}
& \int_0^\infty ds \langle \hat{H}_{\text{int}}(t) \hat{H}_{\text{int}}(t-s) \hat{\rho}_d(t) \rangle_g \\
&= \hbar^2 \int_0^\infty ds \sum_l \mathcal{C}_{\omega_l^g}^2 \left[\hat{a}_1^{\dagger 2} \hat{a}_1^2 \hat{\rho}_d(t) (1 + \bar{n}_l) e^{-i(2\omega_l^g - 2\omega_c)s} \right. \\
&\quad \left. - \hat{a}_1^2 \hat{a}_1^{\dagger 2} \hat{\rho}_d(t) (1 + \bar{n}_l) e^{-i4\omega_c t} e^{i(2\omega_l^g - 2\omega_c)s} \right. \\
&\quad \left. + \hat{a}_1^2 \hat{a}_1^{\dagger 2} \hat{\rho}_d(t) \bar{n}_l e^{-i(2\omega_c - 2\omega_l^g)s} \right. \\
&\quad \left. - \hat{a}_1^{\dagger 2} \hat{a}_1^{\dagger 2} \hat{\rho}_d(t) \bar{n}_l e^{i4\omega_c t} e^{-i(2\omega_c - 2\omega_l^g)s} \right]. \tag{B2}
\end{aligned}$$

Assuming a dense distribution of reservoir modes with density $f(\omega_l^g)$, the sum \sum_l can be replaced by an integral $\int d\omega_l^g f(\omega_l^g)$. Using the Markov approximation and performing the s -integration, we get

$$\begin{aligned}
& \int_0^\infty ds \langle \hat{H}_{\text{int}}(t) \hat{H}_{\text{int}}(t-s) \hat{\rho}_d(t) \rangle_g \\
&= \frac{\pi}{2} \hbar^2 f(\omega_c) C_{\omega_c}^2 \left[(1 + \bar{n}_c) (\hat{a}_1^{\dagger 2} \hat{a}_1^2 \hat{\rho}_d(t) - \hat{a}_1^2 \hat{a}_1^{\dagger 2} \hat{\rho}_d(t) e^{-i4\omega_c t}) \right. \\
&\quad \left. + \bar{n}_c (\hat{a}_1^2 \hat{a}_1^{\dagger 2} \hat{\rho}_d(t) - \hat{a}_1^{\dagger 2} \hat{a}_1^{\dagger 2} \hat{\rho}_d(t) e^{i4\omega_c t}) \right]. \tag{B3}
\end{aligned}$$

Similarly, the other correlation terms appearing in the right-hand side of Eq. (24) are

$$\begin{aligned}
& \int_0^\infty ds \langle \hat{H}_{\text{int}}(t) \hat{\rho}_d(t) \hat{H}_{\text{int}}(t-s) \rangle_g^* \\
&= \frac{\pi}{2} \hbar^2 f(\omega_c) C_{\omega_c}^2 \left[\bar{n}_c (\hat{a}_1^{\dagger 2} \hat{\rho}_d(t) \hat{a}_1^2 - \hat{a}_1^2 \hat{\rho}_d(t) \hat{a}_1^{\dagger 2} e^{-i4\omega_c t}) \right. \\
&\quad \left. + (1 + \bar{n}_c) (\hat{a}_1^2 \hat{\rho}_d(t) \hat{a}_1^{\dagger 2} - \hat{a}_1^{\dagger 2} \hat{\rho}_d(t) \hat{a}_1^{\dagger 2} e^{i4\omega_c t}) \right], \tag{B4}
\end{aligned}$$

$$\begin{aligned}
& \int_0^\infty ds \langle \hat{H}_{\text{int}}(t-s) \hat{\rho}_d(t) \hat{H}_{\text{int}}(t) \rangle_g^* \\
&= \frac{\pi}{2} \hbar^2 f(\omega_c) C_{\omega_c}^2 \left[\bar{n}_c (\hat{a}_1^{\dagger 2} \hat{\rho}_d(t) \hat{a}_1^2 - \hat{a}_1^{\dagger 2} \hat{\rho}_d(t) \hat{a}_1^{\dagger 2} e^{i4\omega_c t}) \right. \\
&\quad \left. + (1 + \bar{n}_c) (\hat{a}_1^2 \hat{\rho}_d(t) \hat{a}_1^{\dagger 2} - \hat{a}_1^2 \hat{\rho}_d(t) \hat{a}_1^2 e^{-i4\omega_c t}) \right], \tag{B5}
\end{aligned}$$

$$\begin{aligned}
& \int_0^\infty ds \langle \hat{\rho}_d(t) \hat{H}_{\text{int}}(t-s) \hat{H}_{\text{int}}(t) \rangle_g \\
&= \frac{\pi}{2} \hbar^2 f(\omega_c) C_{\omega_c}^2 \left[(1 + \bar{n}_c) (\hat{\rho}_d(t) \hat{a}_1^{\dagger 2} \hat{a}_1^2 - \hat{\rho}_d(t) \hat{a}_1^{\dagger 2} \hat{a}_1^{\dagger 2} e^{i4\omega_c t}) \right. \\
&\quad \left. + \bar{n}_c (\hat{\rho}_d(t) \hat{a}_1^2 \hat{a}_1^{\dagger 2} - \hat{\rho}_d(t) \hat{a}_1^2 \hat{a}_1^2 e^{-i4\omega_c t}) \right]. \tag{B6}
\end{aligned}$$

Appendix C: Decoherence with an Energy-Relaxation Channel

In this appendix, we extend our analysis by including an energy-relaxation channel in the master equation. Specifically, we modify Eq. (30) with the Lindblad contribution $\gamma \hat{a}_1 \hat{\rho}_d(t) \hat{a}_1^\dagger - \frac{\gamma}{2} \{ \hat{a}_1^\dagger \hat{a}_1, \hat{\rho}_d(t) \}$, where γ is the energy-relaxation rate. The resulting master equation reads

$$\begin{aligned}
\frac{d}{dt} \hat{\rho}_d(t) &= -\frac{i}{\hbar} [\hat{H}_0, \hat{\rho}_d(t)] + \gamma \hat{a}_1 \hat{\rho}_d(t) \hat{a}_1^\dagger - \frac{\gamma}{2} \{ \hat{a}_1^\dagger \hat{a}_1, \hat{\rho}_d(t) \} \\
&\quad - \frac{\pi}{2} f(\omega_c) C_{\omega_c}^2 \left[(1 + \bar{n}_c) \mathcal{D}_+[\hat{\rho}_d(t)] + \bar{n}_c \mathcal{D}_-[\hat{\rho}_d(t)] \right], \tag{C1}
\end{aligned}$$

where the dissipators \mathcal{D}_\pm are defined explicitly as

$$\begin{aligned}
\mathcal{D}_+[\hat{\rho}_d(t)] &= \{ \hat{a}_1^{\dagger 2} \hat{a}_1^2, \hat{\rho}_d(t) \} - 2\hat{a}_1^2 \hat{\rho}_d(t) \hat{a}_1^{\dagger 2} \\
&\quad - \hat{a}_1^2 \hat{a}_1^2 \hat{\rho}_d(t) - \hat{\rho}_d(t) \hat{a}_1^{\dagger 2} \hat{a}_1^{\dagger 2} + \hat{a}_1^2 \hat{\rho}_d(t) \hat{a}_1^2 \\
&\quad + \hat{a}_1^{\dagger 2} \hat{\rho}_d(t) \hat{a}_1^{\dagger 2}, \tag{C2}
\end{aligned}$$

$$\begin{aligned}
\mathcal{D}_-[\hat{\rho}_d(t)] &= \{ \hat{a}_1^2 \hat{a}_1^{\dagger 2}, \hat{\rho}_d(t) \} - 2\hat{a}_1^{\dagger 2} \hat{\rho}_d(t) \hat{a}_1^2 \\
&\quad - \hat{a}_1^{\dagger 2} \hat{a}_1^{\dagger 2} \hat{\rho}_d(t) - \hat{\rho}_d(t) \hat{a}_1^2 \hat{a}_1^2 + \hat{a}_1^{\dagger 2} \hat{\rho}_d(t) \hat{a}_1^2 \\
&\quad + \hat{a}_1^{\dagger 2} \hat{\rho}_d(t) \hat{a}_1^{\dagger 2}. \tag{C3}
\end{aligned}$$

Following Sec. III, we write

$$\frac{d}{dt} \hat{\rho}_d(t) = (\hat{\mathcal{L}}_1 + \hat{\mathcal{L}}_g) \hat{\rho}_d(t), \quad \hat{\mathcal{L}}_1[\hat{\rho}_d] = -\frac{i}{\hbar} [\hat{H}_0, \hat{\rho}_d] + \mathcal{L}_\gamma[\hat{\rho}_d]. \tag{C4}$$

The first-order formal solution is

$$\hat{\rho}_d(t) = e^{\hat{\mathcal{L}}_1 t} \left[1 + \int_0^t d\tau e^{-\hat{\mathcal{L}}_1 \tau} \hat{\mathcal{L}}_g e^{\hat{\mathcal{L}}_1 \tau} \right] \hat{\rho}_d(0). \tag{C5}$$

To leading order in γ , the free evolution operator acts as

$$e^{\hat{\mathcal{L}}_1 t} A = e^{-i\hat{H}_0 t/\hbar} A e^{i\hat{H}_0 t/\hbar} + O(\gamma), \tag{C6}$$

and the matrix elements evolve as

$$\langle n_1 | \hat{\rho}_d(t) | n_2 \rangle = \langle n_1 | \hat{\rho}_d(0) | n_2 \rangle \exp \left[\int_0^t f(n_1, n_2, t') dt' \right] + O(\gamma), \tag{C7}$$

with

$$f(n_1, n_2, t) = -\frac{i}{\hbar} (E_1 - E_2) - \frac{\gamma}{2} (n_1 + n_2). \tag{C8}$$

1. Examples

For an initial superposition $\hat{\rho}_d(0) = \frac{1}{2}(|0\rangle + |1\rangle)(\langle 0| + \langle 1|)$,

$$\langle 0|\hat{\rho}_d(t)|0\rangle = \frac{1}{2} \left(1 - \frac{t}{\tau_G}\right) + O(\gamma), \quad (\text{C9})$$

$$\langle 1|\hat{\rho}_d(t)|1\rangle = \frac{1}{2} \left(1 - 3\frac{t}{\tau_G}\right) e^{-\gamma t} + O(\gamma), \quad (\text{C10})$$

$$\langle 0|\hat{\rho}_d(t)|1\rangle = \frac{1}{2} \left(1 - 2\frac{t}{\tau_G}\right) e^{i\omega_c t} e^{-\gamma t/2} + O(\gamma), \quad (\text{C11})$$

$$\langle 1|\hat{\rho}_d(t)|0\rangle = \frac{1}{2} \left(1 - 2\frac{t}{\tau_G}\right) e^{-i\omega_c t} e^{-\gamma t/2} + O(\gamma). \quad (\text{C12})$$

For the initially excited state $\hat{\rho}_d(0) = |2\rangle\langle 2|$,

$$\langle 2|\hat{\rho}_d(t)|2\rangle = [1 - 2\pi f(\omega_c) C_{\omega_c}^2 t(1 + 7\bar{n}_c)] e^{-2\gamma t} + O(\gamma). \quad (\text{C13})$$

2. Extraction of effective decay times

In an experiment, population and coherence decay rates are typically obtained by fitting the measured signals to single exponentials of the form e^{-t/T_1} and e^{-t/T_2} . To connect these experimentally defined quantities with the microscopic parameters (γ, τ_G) appearing in our master equation, we now derive the corresponding relations directly from Eqs. (C10) and (C11).

Population decay. For short evolution times $t \ll \tau_G$ and $\gamma t \ll 1$, Eq. (C10) gives

$$\langle 1|\hat{\rho}_d(t)|1\rangle = \frac{1}{2} \left(1 - 3\frac{t}{\tau_G}\right) e^{-\gamma t} + O(t^2). \quad (\text{C14})$$

Using $e^{-\gamma t} = 1 - \gamma t + O(t^2)$, we obtain

$$\begin{aligned} \langle 1|\hat{\rho}_d(t)|1\rangle &= \frac{1}{2} [(1 - 3t/\tau_G)(1 - \gamma t)] + O(t^2) \\ &= \frac{1}{2} \left[1 - \left(\gamma + \frac{3}{\tau_G}\right)t + O(t^2)\right]. \end{aligned} \quad (\text{C15})$$

A single exponential fitted to this decay obeys $e^{-t/T_1} = 1 - t/T_1 + O(t^2)$. Matching the linear terms in t between Eqs. (C15) and e^{-t/T_1} yields

$$T_1^{-1} = \gamma + \frac{3}{\tau_G}. \quad (\text{C16})$$

Coherence decay. Similarly, Eq. (C11) gives for the magnitude of the coherence

$$|\langle 0|\hat{\rho}_d(t)|1\rangle| = \frac{1}{2} \left(1 - 2\frac{t}{\tau_G}\right) e^{-\gamma t/2} + O(t^2). \quad (\text{C17})$$

Expanding $e^{-\gamma t/2} = 1 - \frac{\gamma}{2}t + O(t^2)$ and multiplying out,

$$\begin{aligned} |\langle 0|\hat{\rho}_d(t)|1\rangle| &= \frac{1}{2} \left[(1 - 2t/\tau_G) \left(1 - \frac{\gamma}{2}t\right)\right] + O(t^2) \\ &= \frac{1}{2} \left[1 - \left(\frac{\gamma}{2} + \frac{2}{\tau_G}\right)t + O(t^2)\right]. \end{aligned} \quad (\text{C18})$$

The Ramsey-envelope fit has the form $e^{-t/T_2} = 1 - t/T_2 + O(t^2)$. Matching linear coefficients gives

$$T_2^{-1} = \frac{\gamma}{2} + \frac{2}{\tau_G}. \quad (\text{C19})$$

Eqs. (C16) and (C19) show that the experimentally accessible decay times (T_1, T_2) encode two independent linear combinations of the intrinsic damping rate γ and the gravitationally induced decoherence rate $1/\tau$. Consequently, simultaneous measurement of (T_1, T_2) allows one to solve for (γ, τ) uniquely. In particular, in the quantum-vacuum case the coefficients (3, 2) imply that the $\{|0\rangle, |1\rangle\}$ subspace is partially protected against gravitational decoherence, whereas in the classical stochastic case the same subspace decoheres at a rate proportional to $1/\tau_\alpha$. This provides a clear experimental discriminant between quantum and classical gravitational-wave backgrounds.

Appendix D: Generalized coherent states

In the main text, in order to model the classical limit of gravitationally induced decoherence, we chose to work with an ensemble of phase-randomized coherent states, as defined in Eq. (53). This choice was made primarily for calculational simplicity and to allow a transparent one-to-one correspondence with the fully quantum treatment. Importantly, however, the physical conclusions of our analysis do not rely on the phase randomization itself.

Indeed, one may equally well consider a generalized multimode coherent state of the gravitational field, in which the graviton density matrix is taken to be a pure product state,

$$\rho_g \rightarrow \rho_g^{\text{ch}} = \bigotimes_k |\alpha_k\rangle\langle\alpha_k|, \quad \alpha_k = |\alpha_k| e^{i\phi_k}, \quad (\text{D1})$$

with fixed (but otherwise arbitrary) phases ϕ_k .

Adopting this description modifies the graviton bilinear expectation values entering the master equation. In particular, the relations in Eqs. (55) are replaced by

$$\begin{aligned} \langle \hat{b}_l^\dagger \hat{b}_m^\dagger \rangle_g^\alpha &= \alpha_l^* \alpha_m^*, & \langle \hat{b}_l^\dagger \hat{b}_m \rangle_g^\alpha &= \alpha_l^* \alpha_m, \\ \langle \hat{b}_l \hat{b}_m^\dagger \rangle_g^\alpha &= \delta_{lm} + \alpha_l \alpha_m^*, & \langle \hat{b}_l \hat{b}_m \rangle_g^\alpha &= \alpha_l \alpha_m, \\ \langle \hat{b}_l^\dagger \hat{b}_m^\dagger \rangle_g^{*\alpha} &= \alpha_l^* \alpha_m^*, & \langle \hat{b}_l^\dagger \hat{b}_m \rangle_g^{*\alpha} &= \delta_{lm} + \alpha_l^* \alpha_m, \\ \langle \hat{b}_l \hat{b}_m^\dagger \rangle_g^{*\alpha} &= \alpha_l \alpha_m^*, & \langle \hat{b}_l \hat{b}_m \rangle_g^{*\alpha} &= \alpha_l \alpha_m. \end{aligned} \quad (\text{D2})$$

Using these relations instead of Eqs. (55) leads to a master equation that is algebraically more involved than Eq. (56). Nevertheless, its overall structure remains unchanged: the reduced dynamics of the detector (Eqs. (24)) can still be written as the sum of a vacuum contribution and a coherent-state-dependent contribution,

$$\dot{\rho}_d = \dot{\rho}_d^{\text{vac}} + \dot{\rho}_d^{(\alpha)}. \quad (\text{D3})$$

The vacuum contribution originates from the δ_{km} term in $\langle \hat{b}_k \hat{b}_m^\dagger \rangle_g$ and gives rise to the genuine Lindblad dissipator

$$\begin{aligned} \dot{\rho}_d^{\text{vac}} = & \Gamma (a^2 \rho_d a^{\dagger 2} - \frac{1}{2} \{a^{\dagger 2} a^2, \rho_d\}) \\ & - \hat{a}_1^2 \hat{a}_1^\dagger \hat{\rho}_d(t) e^{-i4\omega_c t} - \hat{\rho}_d(t) \hat{a}_1^{\dagger 2} \hat{a}_1^2 e^{i4\omega_c t} + \hat{a}_1^\dagger \hat{\rho}_d(t) \hat{a}_1^2 e^{-i4\omega_c t} \\ & + \hat{a}_1^{\dagger 2} \hat{\rho}_d(t) e^{i4\omega_c t} \hat{a}_1^2, \end{aligned} \quad (\text{D4})$$

with $\Gamma = 2\pi f(\omega_c) C_{\omega_c}^2$.

The α -dependent contribution takes the form

$$\begin{aligned} \dot{\rho}_d^{(\alpha)}(t) = & |\alpha_{\omega_c}|^2 \sum_k \left[e^{+i\Delta_k t} (a^{\dagger 2} \rho_d a^2 - a^2 a^{\dagger 2} \rho_d) \right. \\ & \left. + e^{-i\Delta_k t} (a^2 \rho_d a^{\dagger 2} - \rho_d a^{\dagger 2} a^2) \right]. \end{aligned} \quad (\text{D5})$$

with

$$\Delta_k = 2(\omega_c - \omega_k). \quad (\text{D6})$$

Crucially, all α -dependent terms are purely oscillatory in time. Upon performing the long-time (secular) average,

$$\frac{1}{T} \int_t^{t+T} dt' e^{\pm i\Delta t'} \xrightarrow{T \rightarrow \infty} 0, \quad (\text{D7})$$

these contributions vanish identically. Consequently, a purely coherent gravitational-wave background with fixed phase does not induce decoherence in the detector, and the reduced evolution remains unitary.

Decoherence therefore arises solely from vacuum graviton fluctuations or from genuinely stochastic gravitational-wave backgrounds, such as those described by phase-randomized coherent states.

Appendix E: Spontaneous Graviton Emission and Consistency of the Born–Markov Approximation

In deriving the master equation we have employed the Born–Markov approximation,

$$\rho_{\text{tot}}(t) \approx \rho_d(t) \otimes \rho_g, \quad (\text{E1})$$

where the gravitational bath is assumed to remain in its initial state ρ_g , taken to be the vacuum. Since the detector–gravity interaction permits spontaneous graviton emission, it is necessary to verify that this factorization remains self-consistent.

Consider the transition

$$|i\rangle = |2\rangle \otimes |0_g\rangle \longrightarrow |f\rangle = |0\rangle \otimes |1_k\rangle, \quad (\text{E2})$$

in which the detector loses energy $2\hbar\omega_c$ while emitting a graviton of energy $\hbar\omega_k$. Energy conservation requires

$$2\hbar\omega_c = \hbar\omega_k, \quad \omega_k = 2\omega_c. \quad (\text{E3})$$

For the interaction Hamiltonian

$$\begin{aligned} H_{\text{int}} = & \hbar \sum_k C_{\omega_k^g} \left[e^{i\omega_k^g t} b_k^\dagger (\hat{a}_1^{\dagger 2} - \hat{a}_1^2) \right. \\ & \left. - e^{-i\omega_k^g t} b_k (\hat{a}_1^{\dagger 2} - \hat{a}_1^2) \right]. \end{aligned} \quad (\text{E4})$$

the relevant matrix element is

$$\langle 0, 1_k | H_{\text{int}} | 2, 0 \rangle. \quad (\text{E5})$$

Using

$$a^2 |2\rangle = \sqrt{2} |0\rangle, \quad b_k^\dagger |0\rangle = |1_k\rangle, \quad (\text{E6})$$

one obtains

$$|\langle f | H_{\text{int}} | i \rangle|^2 = 2\hbar^2 C_{\omega_k^g}^2. \quad (\text{E7})$$

Replacing the discrete mode sum by the continuum prescription used in the main text,

$$\sum_k \rightarrow \frac{V}{2\pi^2} \int_0^\infty d\omega_g f(\omega_g), \quad (\text{E8})$$

the spontaneous graviton emission rate in the long-time limit can be derived using Fermi’s Golden Rule. Here the “long-time limit” refers to times large compared to the correlation time of the gravitational reservoir, so that the oscillatory time integrals generate an energy-conserving delta function. Importantly, this limit does *not* require times comparable to the system lifetime, but only $t \gg \tau_{\text{bath}}$, where τ_{bath} denotes the decay time of the bath two-point correlation function.

Under this condition one obtains

$$\gamma_{\text{em}} = \frac{2\pi}{\hbar} |\langle f | H_{\text{int}} | i \rangle|^2 f(\omega_k), \quad (\text{E9})$$

which yields

$$\gamma_{\text{em}} = \frac{2\hbar}{\pi} C_{\omega_k^g}^2 f(2\omega_c). \quad (\text{E10})$$

For gravitational interactions one has $\tau_{\text{bath}} \ll \tau_G$ by many orders of magnitude, so there exists a broad intermediate regime $\tau_{\text{bath}} \ll t \ll \tau_G$ in which both the Golden-Rule treatment and the perturbative Born–Markov approximation are simultaneously valid.

In our model, the coupling coefficient satisfies

$$C_\omega^2 = \frac{\omega \ell_p^2}{2} = \frac{\hbar G \omega}{2c^3}. \quad (\text{E11})$$

For free gravitons in 3 + 1 dimensions, the density of modes obeys $f(\omega) \propto \omega^2$. Consequently,

$$\gamma_{\text{em}} \sim \omega_c \left(\frac{\omega_c}{\omega_{\text{Pl}}} \right)^2, \quad (\text{E12})$$

where $\omega_{\text{Pl}} = \sqrt{c^5/(\hbar G)}$ denotes the Planck angular frequency. For any laboratory mechanical frequency $\omega_c \ll$

ω_{P1} , the factor $(\omega_c/\omega_{P1})^2$ renders the emission rate negligibly small.

Initially the gravitational field is in the vacuum state,

$$\langle b_k^\dagger b_k \rangle_{t=0} = 0. \quad (\text{E13})$$

In the weak-coupling regime the emission probability grows linearly,

$$P_{\text{emit}}(t) = \gamma_{\text{em}} t. \quad (\text{E14})$$

Since $\gamma_{\text{em}} t \ll 1$ for all experimentally relevant times, the probability distribution satisfies

$$P(0) \simeq 1 - \gamma_{\text{em}} t, \quad P(1) \simeq \gamma_{\text{em}} t, \quad P(n \geq 2) \approx 0. \quad (\text{E15})$$

The average graviton occupation therefore obeys

$$\langle b_k^\dagger b_k \rangle = \gamma_{\text{em}} t \ll 1. \quad (\text{E16})$$

Thus, although spontaneous graviton emission is permitted by the interaction Hamiltonian, the detector-induced modification of the gravitational bath remains perturbatively small. The Born approximation does not require the absence of emission, but only that the bath state remain effectively unchanged to leading order. Since $\gamma_{\text{em}} t \ll 1$, system–bath correlations are of higher order in the coupling, and the Born–Markov treatment employed in the main text is self-consistent.

-
- [1] B. P. Abbott, *et al.* (LIGO Scientific Collaboration, and V. Collaboration), *Phys. Rev. Lett.* **116**, 061102 (2016).
- [2] R. Abbott *et al.* (KAGRA, VIRGO, LIGO Scientific), *Phys. Rev. X* **13**, 041039 (2023), [arXiv:2111.03606 \[gr-qc\]](#).
- [3] J. Foo, R. B. Mann, and M. Zych, *arXiv preprint* (2025), [arXiv:2302.03259 \[gr-qc\]](#).
- [4] S. K. Manikandan and F. Wilczek, *Phys. Rev. A* **111**, 033705 (2025).
- [5] S. K. Manikandan and F. Wilczek, *Int. J. Mod. Phys. D* **34**, 2543001 (2025), [arXiv:2505.11407 \[gr-qc\]](#).
- [6] S. K. Manikandan and F. Wilczek, *Phys. Rev. A* **112**, 043716 (2025), [arXiv:2505.11422 \[gr-qc\]](#).
- [7] S. Marti, U. von Lüpkke, O. Joshi, Y. Yang, M. Bild, A. Omahen, Y. Chu, and M. Fadel, *Nature Phys.* **20**, 1448 (2024), [arXiv:2312.16169 \[quant-ph\]](#).
- [8] H.-P. Breuer and F. Petruccione, *The Theory of Open Quantum Systems* (Oxford University Press, New York, 2006).
- [9] G. Ghosh, B. Dutta-Roy, and M. Dey, *Journal of Physics G: Nuclear Physics* **3**, 1077 (1977).
- [10] P. Nandi, T. Bhattacharyya, A. S. Majumdar, G. Pleasance, and F. Petruccione, *Phys. Rev. Research* (2025), [arXiv:2503.13061 \[hep-th\]](#).
- [11] P. Nandi and F. Petruccione, “Quantum openness of the universe: Emergent dark matter and dark energy,” In preparation.
- [12] P. Nandi, P. Ghose, and F. Petruccione, (2025), [arXiv:2510.10836 \[gr-qc\]](#).
- [13] C. Zhang, *Phys. Rev. D* **112**, 104022 (2025), [arXiv:2511.21403 \[gr-qc\]](#).
- [14] D. Miki, A. Matsumura, and K. Yamamoto, *Phys. Rev. D* **103**, 026017 (2021).
- [15] T. Guerreiro, *Phys. Rev. D* **112**, L101904 (2025), [arXiv:2501.17043 \[gr-qc\]](#).
- [16] Y. Kaku and Y. Nambu, *Phys. Rev. D* **111**, 046026 (2025), [arXiv:2411.12997 \[gr-qc\]](#).
- [17] P. Jones, Q. G. Bailey, A. Gretarsson, and E. Poon, *Phys. Lett. B* **868**, 139628 (2025), [arXiv:2411.15632 \[gr-qc\]](#).
- [18] F.-L. Lin and S. Mondal, (2025), [arXiv:2510.23584 \[hep-th\]](#).
- [19] T. P. Singh and T. Padmanabhan, *Physical Review D* **35**, 2993 (1987).
- [20] S. M. e. a. Aston, *Update on Quadruple Suspension Design for Advanced LIGO*, Tech. Rep. LIGO-P1200056-v3 (LIGO Scientific Collaboration, 2012).
- [21] D. Sigg, *Gravitational Waves (A Review of LIGO)*, Tech. Rep. LIGO-P980007-00-D (LIGO, 1998).
- [22] P. Nandi and B. R. Majhi, *Phys. Lett. B* **857**, 138988 (2024), [arXiv:2403.11253 \[gr-qc\]](#).
- [23] P. Nandi, B. R. Majhi, N. Debnath, and S. Kala, *Phys. Lett. B* **853**, 138706 (2024), [arXiv:2401.02778 \[gr-qc\]](#).
- [24] A. Arvanitaki and A. A. Geraci, *Phys. Rev. Lett.* **110**, 071105 (2013).
- [25] A. D. O’Connell, M. Hofheinz, M. Ansmann, R. C. Bialczak, M. Lenander, E. Lucero, M. Neeley, D. Sank, H. Wang, M. Weides, J. Wenner, J. M. Martinis, and A. N. Cleland, *Nature* **464**, 697 (2010).
- [26] J. D. Teufel, T. Donner, D. Li, J. W. Harlow, M. S. Allman, K. Cicak, A. J. Sirois, J. D. Whittaker, R. W. Simmonds, and K. W. Lehnert, *Nature* **475**, 359 (2011).
- [27] Y. Chu, T. P. M. Alegre, A. H. Safavi-Naeini, J. T. Hill, A. Krause, S. Gröblacher, M. Aspelmeyer, and O. Painter, *Nature* **478**, 89 (2011).
- [28] D. Miki, A. Matsumura, and K. Yamamoto, *Phys. Rev. D* **109**, 064090 (2024), [arXiv:2311.00563 \[gr-qc\]](#).
- [29] C. Wan, *Quantum Superposition on Nano-Mechanical Oscillator*, Ph.d. thesis, Imperial College London (2017).
- [30] Y. Chu, P. Kharel, W. H. Renninger, L. D. Burkhardt, L. Frunzio, P. T. Rakich, and R. J. Schoelkopf, *Science* **358**, 199 (2017), [arXiv:1703.00342 \[quant-ph\]](#).
- [31] S. Donadi and M. Fadel, *Phys. Rev. D* **111**, 026009 (2025).
- [32] P. Nandi, S. Pal, S. K. Pal, and B. R. Majhi, *Phys. Rev. D* **108**, 124069 (2023), [arXiv:2207.08687 \[gr-qc\]](#).
- [33] M. Dutta, P. Nandi, and B. R. Majhi, *JHEP* **08**, 104 (2025), [arXiv:2503.19688 \[gr-qc\]](#).
- [34] M. Dutta, P. Nandi, and B. R. Majhi, (2025), [arXiv:2510.11075 \[gr-qc\]](#).
- [35] H.-T. Cho and B.-L. Hu, *Phys. Rev. D* **105**, 086004 (2022), [arXiv:2112.08174 \[gr-qc\]](#).
- [36] K. Bhattacharya, S. Mohanty, and A. Nautiyal, *Phys. Rev. Lett.* **97**, 251301 (2006).
- [37] M. P. Blencowe, *Phys. Rev. Lett.* **111**, 021302 (2013).
- [38] I. Antoniou, D. Papadopoulos, and L. Perivolaropoulos,

- Physical Review D **94**, 084018 (2016).
- [39] M. Maggiore, *Gravitational Waves: Theory and Experiment*, Vol. 1 (Oxford University Press, New York, 2008).
- [40] C. W. Misner, K. S. Thorne, and J. A. Wheeler, *Gravitation* (W. H. Freeman and Company, San Francisco, 1973).
- [41] C. R. Galley, R. O. Behunin, and B. L. Hu, *Phys. Rev. A* **87**, 043832 (2013).
- [42] M. Parikh, F. Wilczek, and G. Zahariade, *Phys. Rev. D* **104**, 046021 (2021), [arXiv:2010.08208 \[hep-th\]](#).
- [43] A. D. Speliotopoulos, *Phys. Rev. D* **51**, 1701 (1995).
- [44] M. Parikh, F. Wilczek, and G. Zahariade, *Phys. Rev. Lett.* **127**, 081602 (2021).
- [45] A. Saha, S. Gangopadhyay, and S. Saha, *Phys. Rev. D* **97**, 044015 (2018).
- [46] U. von Lüpke, Y. Yang, M. Bild, L. Michaud, M. Fadel, and Y. Chu, *Nature Physics* **18**, 794 (2022).
- [47] M. Aspelmeyer, T. J. Kippenberg, and F. Marquardt, *Rev. Mod. Phys.* **86**, 1391 (2014).
- [48] D. Vitali, S. Gigan, A. Ferreira, H. R. Böhm, P. Tombesi, A. Guerreiro, V. Vedral, A. Zeilinger, and M. Aspelmeyer, *Phys. Rev. Lett.* **98**, 030405 (2007).
- [49] U. Delić, M. Reisenbauer, K. Dare, D. Grass, V. Vuletić, N. Kiesel, and M. Aspelmeyer, *Science* **367**, 892 (2020), [arXiv:1911.04406 \[quant-ph\]](#).
- [50] D. Barman, S. Barman, and B. R. Majhi, *JHEP* **07**, 124 (2021), [arXiv:2104.11269 \[gr-qc\]](#).
- [51] G. S. Agarwal, R. R. Puri, and R. P. Singh, *Phys. Rev. A* **56**, 2249 (1997).
- [52] A. O. Caldeira and A. J. Leggett, *Physica A* **121**, 587 (1983).
- [53] B. Ghayour, *Gravitational Waves in Thermal States*, Ph.d. thesis, University of Hyderabad, Hyderabad, India (2012).
- [54] N. D. Birrell and P. C. W. Davies, *Quantum Fields in Curved Space* (Cambridge University Press, 1982).
- [55] J. C. Botke, D. J. Scalapino, and R. L. Sugar, *Physical Review D* **9**, 813 (1974).
- [56] S. Kanno, J. Soda, and A. Taniguchi, *Phys. Rev. Lett.* **136**, 061404 (2026).
- [57] D. Bhaumik, K. Bhaumik, and B. Dutta-Roy, *Journal of Physics A: Mathematical and General* **9**, 1507 (1976).
- [58] R. Gomatam, *Physical Review D* **3**, 2169 (1971).
- [59] U. von Lüpke, Y. Yang, M. Bild, L. Michaud, M. Fadel, and Y. Chu, *Nature Physics* **18**, 794 (2022).
- [60] S. Marti, U. von Lüpke, O. Joshi, Y. Yang, M. Bild, A. Omahen, Y. Chu, and M. Fadel, *Nature Physics* **20**, 1448 (2024).
- [61] B. Schriniski, Y. Yang, U. von Lüpke, M. Bild, Y. Chu, K. Hornberger, S. Nimmrichter, and M. Fadel, *Phys. Rev. Lett.* **130**, 133604 (2023).
- [62] A. Ito, J. Soda, and M. Yamaguchi, *JCAP* **03**, 033 (2021), [arXiv:2009.03611 \[astro-ph.CO\]](#).
- [63] Y. Kahn, J. Schütte-Engel, and T. Trickle, *Phys. Rev. D* **109**, 096023 (2024).
- [64] S. Kanno, J. Soda, and A. Taniguchi, *Eur. Phys. J. C* **85**, 31 (2025), [arXiv:2311.03890 \[gr-qc\]](#).
- [65] M. Maggiore, *Phys. Rept.* **331**, 283 (2000), [arXiv:gr-qc/9909001](#).
- [66] Y. Ema, R. Jinno, and K. Nakayama, *JCAP* **09**, 015 (2020), [arXiv:2006.09972 \[astro-ph.CO\]](#).
- [67] V. Domcke and C. Garcia-Cely, *Phys. Rev. Lett.* **126**, 021104 (2021), [arXiv:2006.01161 \[astro-ph.CO\]](#).
- [68] A. J. R. MacDonald, B. D. Hauer, X. Rojas, P. H. Kim, G. G. Popowich, and J. P. Davis, *Phys. Rev. A* **93**, 013836 (2016).
- [69] L. Li, X. Ruan, S.-L. Zhao, *et al.*, *Phys. Rev. Appl.* **24**, 064064 (2025).
- [70] M. Toroš, A. Mazumdar, and S. Bose, *Phys. Rev. D* **109**, 084050 (2024).
- [71] S. Sen, S. Gangopadhyay, and S. Bhattacharyya, *Phys. Rev. D* **110**, 026008 (2024).
- [72] A. Das, M. Parikh, F. Wilczek, and R. Wutte, (2025), [arXiv:2512.20601 \[gr-qc\]](#).